Fast-transient Searches in Real Time with ZTFReST: Identification of Three Optically Discovered Gamma-Ray Burst Afterglows and New Constraints on the Kilonova Rate

Igor Andreoni[1] ⓘ, Michael W. Coughlin[2] ⓘ, Erik C. Kool[3] ⓘ, Mansi M. Kasliwal[1] ⓘ, Harsh Kumar[4], Varun Bhalerao[4] ⓘ,
Ana Sagués Carracedo[5] ⓘ, Anna Y. Q. Ho[6,7,8] ⓘ, Peter T. H. Pang[9,10], Divita Saraogi[4], Kritti Sharma[4] ⓘ, Vedant Shenoy[4],
Eric Burns[11], Tomás Ahumada[12] ⓘ, Shreya Anand[1] ⓘ, Leo P. Singer[13,14] ⓘ, Daniel A. Perley[15] ⓘ, Kishalay De[1], U. C. Fremling[1],
Eric C. Bellm[16] ⓘ, Mattia Bulla[3] ⓘ, Arien Crellin-Quick[6], Tim Dietrich[17,18] ⓘ, Andrew Drake[1], Dmitry A. Duev[1] ⓘ,
Ariel Goobar[5] ⓘ, Matthew J. Graham[1] ⓘ, David L. Kaplan[19] ⓘ, S. R. Kulkarni[1] ⓘ, Russ R. Laher[20] ⓘ, Ashish A. Mahabal[1,21] ⓘ,
David L. Shupe[20] ⓘ, Jesper Sollerman[3] ⓘ, Richard Walters[22], and Yuhan Yao[1] ⓘ

[1] Division of Physics, Mathematics and Astronomy, California Institute of Technology, Pasadena, CA 91125, USA; andreoni@caltech.edu
[2] School of Physics and Astronomy, University of Minnesota, Minneapolis, MN 55455, USA; cough052@umn.edu
[3] The Oskar Klein Centre, Department of Astronomy, Stockholm University, AlbaNova, SE-106 91 Stockholm, Sweden
[4] Indian Institute of Technology Bombay, Powai, Mumbai 400076, India
[5] The Oskar Klein Centre, Department of Physics, Stockholm University, AlbaNova, SE-106 91 Stockholm, Sweden
[6] Department of Astronomy, University of California, Berkeley, CA 94720-3411, USA
[7] Lawrence Berkeley National Laboratory, 1 Cyclotron Road, MS 50B-4206, Berkeley, CA 94720, USA
[8] Miller Institute for Basic Research in Science, 468 Donner Lab, Berkeley, CA 94720, USA
[9] Nikhef, 1098 XG Amsterdam, The Netherlands
[10] Department of Physics, Utrecht University, 3584 CC Utrecht, The Netherlands
[11] Department of Physics and Astronomy, Louisiana State University, Baton Rouge, LA 70803, USA
[12] Department of Astronomy, University of Maryland, College Park, MD 20742, USA
[13] Astrophysics Science Division, NASA Goddard Space Flight Center, MC 661, Greenbelt, MD 20771, USA
[14] Joint Space-Science Institute, University of Maryland, College Park, MD 20742, USA
[15] Astrophysics Research Institute, Liverpool John Moores University, IC2, Liverpool Science Park, 146 Brownlow Hill, Liverpool L3 5RF, UK
[16] DIRAC Institute, Department of Astronomy, University of Washington, 3910 15th Avenue NE, Seattle, WA 98195, USA
[17] Institut für Physik und Astronomie, Universität Potsdam, D-14476 Potsdam, Germany
[18] Max Planck Institute for Gravitational Physics (Albert Einstein Institute), Am Mühlenberg 1, Potsdam D-14476, Germany
[19] Center for Gravitation, Cosmology and Astrophysics, Department of Physics, University of Wisconsin–Milwaukee, P.O. Box 413, Milwaukee, WI 53201, USA
[20] IPAC, California Institute of Technology, 1200 E. California Boulevard, Pasadena, CA 91125, USA
[21] Center for Data Driven Discovery, California Institute of Technology, Pasadena, CA 91125, USA
[22] Caltech Optical Observatories, California Institute of Technology, Pasadena, CA 91125, USA

Abstract

The most common way to discover extragalactic fast transients, which fade within a few nights in the optical, is via follow-up of gamma-ray burst and gravitational-wave triggers. However, wide-field surveys have the potential to identify rapidly fading transients independently of such external triggers. The volumetric survey speed of the Zwicky Transient Facility (ZTF) makes it sensitive to objects as faint and fast fading as kilonovae, the optical counterparts to binary neutron star mergers, out to almost 200 Mpc. We introduce an open-source software infrastructure, the ZTF REaltime Search and Triggering, ZTFReST, designed to identify kilonovae and fast transients in ZTF data. Using the ZTF alert stream combined with forced point-spread-function photometry, we have implemented automated candidate ranking based on their photometric evolution and fitting to kilonova models. Automated triggering, with a human in the loop for monitoring, of follow-up systems has also been implemented. In 13 months of science validation, we found several extragalactic fast transients independently of any external trigger, including two supernovae with post-shock cooling emission, two known afterglows with an associated gamma-ray burst (ZTF20abbiixp, ZTF20abwysqy), two known afterglows without any known gamma-ray counterpart (ZTF20aajnksq, ZTF21aaeyldq), and three new fast-declining sources (ZTF20abtxwfx, ZTF20acozryr, ZTF21aagwbjr) that are likely associated with GRB200817A, GRB201103B, and GRB210204A. However, we have not found any objects that appear to be kilonovae. We constrain the rate of GW170817-like kilonovae to $R < 900 \, \mathrm{Gpc}^{-3} \, \mathrm{yr}^{-1}$ (95% confidence). A framework such as ZTFReST could become a prime tool for kilonova and fast-transient discovery with the Vera Rubin Observatory.

Unified Astronomy Thesaurus concepts: Transient detection (1957); Transient sources (1851); Optical astronomy (1776); Gamma-ray bursts (629); Neutron stars (1108)

Supporting material: data behind figures

1. Introduction

Multi-messenger sources of astrophysical transients are changing time-domain astronomy. With a variety of survey facilities now online, there are numerous examples of systems making detections of these sources in the optical possible. These include the Panoramic Survey Telescope and Rapid Response System (Pan-STARRS; Morgan et al. 2012), Asteroid Terrestrial-impact Last Alert System (ATLAS; Tonry et al. 2018), the Dark Energy Camera (DECam; Flaugher et al. 2015), the Zwicky Transient Facility (ZTF; Bellm et al. 2019; Graham et al. 2019; Masci et al. 2019; Dekany et al. 2020), and in the near future, BlackGEM (Bloemen et al. 2015), and the Vera C. Rubin Observatory's Legacy Survey of Space and Time (LSST; Ivezić et al. 2019).

Relevant for optical fast-transient discovery have been searches for afterglows from gamma-ray bursts (GRBs; Klebesadel et al. 1973; Metzger et al. 1997; Gehrels & Mészáros 2012); these include both *short* and *long* classes (Kouveliotou et al. 1993), although this classification is subject to debate (Norris & Bonnell 2006; Zhang 2008; Bromberg et al. 2013; Burns et al. 2016). These sources have been identified by GRB survey instruments such as the Neil Gehrels Swift Observatory mission (Gehrels et al. 2004) and the Gamma-ray Burst Monitor (GBM; Meegan et al. 2009) on board the Fermi satellite. In addition to many afterglow detections associated with Swift, dedicated follow-up of GBM sources in particular by both the Palomar Transient Factory (PTF; Law et al. 2009) and ZTF at Palomar Observatory have yielded afterglow detections as well (Singer et al. 2015; Coughlin et al. 2019b; T. Ahumada et al. 2021, in preparation).

During LIGO and Virgo's second observing run, the detection of GW170817 (Abbott et al. 2017b), its burst of gamma-rays GRB 170817A (Goldstein et al. 2017; Savchenko et al. 2017; Abbott et al. 2017c), its short GRB afterglow (Alexander et al. 2017; Haggard et al. 2017; Hallinan et al. 2017; Margutti et al. 2017; Troja et al. 2017), and an optical/infrared *kilonova* counterpart, AT2017gfo (Andreoni et al. 2017; Arcavi et al. 2017; Hu et al. 2017; Chornock et al. 2017; Coulter et al. 2017; Cowperthwaite et al. 2017; Drout et al. 2017; Díaz et al. 2017; Evans et al. 2017; Kasliwal et al. 2017; Kilpatrick et al. 2017; Lipunov et al. 2017; McCully et al. 2017; Nicholl et al. 2017; Shappee et al. 2017; Pian et al. 2017; Smartt et al. 2017; Tanvir et al. 2017; Utsumi et al. 2017), introduced the world to the science of counterparts to gravitational waves (GWs) detected by Advanced LIGO (Aasi et al. 2015), Advanced Virgo (Acernese et al. 2015), and in the future, Kamioka Gravitational Wave Detector (KAGRA; Somiya 2012). The detection and characterization of kilonovae enable constraints on the neutron star equation of state (Bauswein et al. 2017; Margalit & Metzger 2017; Annala et al. 2018; Most et al. 2018; Radice et al. 2018; Coughlin et al. 2018, 2019a, 2019c; Lai et al. 2019; Dietrich et al. 2020), the Hubble constant (Abbott et al. 2017a; Hotokezaka et al. 2019; Coughlin et al. 2020a, 2020b; Dietrich et al. 2020), and r-process nucleosynthesis (Chornock et al. 2017; Coulter et al. 2017; Cowperthwaite et al. 2017; Pian et al. 2017; Rosswog et al. 2017; Smartt et al. 2017; Kasliwal et al. 2019b; Watson et al. 2019).

With the end of the third LIGO-Virgo observing run (O3), and with the entrance of KAGRA, without a viable counterpart to a binary neutron star or neutron star–black hole merger candidate (e.g., Andreoni et al. 2019a; Coughlin et al. 2019d; Goldstein et al. 2019; Gomez et al. 2019; Lundquist et al. 2019; Anand et al. 2020; Ackley et al. 2020; Andreoni et al. 2020b; Antier et al. 2020; Gompertz et al. 2020; Kasliwal et al. 2020), it becomes particularly urgent to continue the search for such objects in optical, wide-field survey data, independently of other multi-messenger and multiwavelength triggers. These searches also serve as unbiased surveys for optical emission, with the potential to discover, for example, collapsars with dirty fireballs (Dermer et al. 2000) that do not have prompt GRB emission (Dermer et al. 2000; Huang et al. 2002; Rhoads 2003), or study whether optically identified kilonovae differ from those identified with gravitational-wave detections, while also enabling many of the studies of both cosmology and nuclear physics identified above. In this work, we will refer to *serendipitous* observations (and discoveries) as those performed within routine survey observations, as opposed to *triggered* target of opportunity (ToO)

observations, which use timing and/or localization information from other wavelengths or messengers.

There are several differences between serendipitous and ToO searches. When a GW, GRB, or neutrino alert is issued, it is possible to perform dedicated, high-cadence ToO observations of these fields, using either a synoptic or a galaxy-targeted strategy (Gehrels et al. 2016). In addition to localization information, a trigger also provides an explosion time to which we can compare all of the transients in the alert stream. Serendipitous observations, on the other hand, do not rely on another detector to have found an astrophysical transient first, and therefore have neither localization nor explosion time information. For this reason, rare fast transients can be more difficult to pick out. Survey data also provide us with a much larger number of images to mine, which is technically challenging, but at the same time could offer a broad range of discovery opportunities. Serendipitous searches of this type have already been successful in the cases of GRB afterglows (Cenko et al. 2015; Stalder et al. 2017; Ho et al. 2018; Andreoni et al. 2020e; Kasliwal et al. 2020) and afterglows with no GRB detected (Cenko et al. 2013; Ho et al. 2020c). Multi-facility programs such as the "Deeper, Wider, Faster" program (Andreoni et al. 2020a; J. Cooke et al. 2021, in preparation) aim discovering counterparts to fast radio bursts and other elusive transients via simultaneous multi-facility observations at many different wavelengths.

We are motivated to search for serendipitous kilonovae in optical survey data. Unfortunately, kilonovae and GRB afterglows, the objective of this study, rapidly fade in the optical (on timescales of a night), and therefore are more difficult to detect than other transients such as supernovae, often identifiable for weeks to months. In addition, kilonovae are expected to rapidly redden with time, making their identification potentially easier but detection possibly harder in optical bands.

There are many more transients from the alert generators than can be characterized in these modes of operation, due to limited follow-up telescope time. For example, ZTF can generate more than a million alert packets per night (Patterson et al. 2018), thus providing the transient community with a preview of the experience expected for the LSST data stream. However, as of 2020 December, only ~10% of transients reported on the Transient Name Server (TNS) have been spectroscopically classified (Kulkarni 2020), predominantly due to lack of observation time. As kilonovae are inherently faint, it is relatively unlikely for them to be classified in routine spectroscopic follow-up of bright transients such as through the Bright Transient Survey (Fremling et al. 2020). Galaxy-targeted searches such as the Census of the Local Universe program (De et al. 2020a) are sensitive to dimmer sources, although the project relies only on ZTF alerts and is limited by galaxy catalog completeness.

In Andreoni et al. (2020b), we presented kilonova rate constraints from archival searches of serendipitous observations from 2018 March to 2020 February. These observations were during ZTF Phase I, which covered 2018 March to 2020 September; ZTF Phase II has been ongoing since then. In Andreoni et al. (2020b), several candidates were identified where real time follow-up with either deeper photometric or spectroscopic resources would have greatly improved our ability to confirm the nature of the fast transients. This fact motivated us to automate discovery and follow-up infrastructure to rapidly identify fast transients in optical survey data; other surveys such

as Pan-STARRS are also undertaking dedicated searches of this kind (McBrien et al. 2020). This infrastructure is inspired by brokers such as the Alert Management, Photometry and Evaluation of Lightcurves (AMPEL; Soumagnac & Ofek 2018; Nordin et al. 2019) and builds upon existing tools such as the Target and Observation Managers being built by Las Cumbres Observatory (LCO) and others (Street et al. 2018), or the automatic triggering capabilities already implemented in AMPEL (Nordin et al. 2019).

We have developed automated filtering and follow-up infrastructure designed to perform a serendipitous search for kilonovae and afterglows known as ZTF Realtime Search and Triggering, ZTFReST. In this paper, we describe the ZTFReST automated infrastructure and first results obtained during science validation. We describe the algorithms and their implementation in Section 2. The science validation and early results are detailed in Section 3. Three case studies are extensively presented in Section 4 to demonstrate the type of multiwavelength analysis made possible when fast transients are found serendipitously in the survey. We translate our non-detection of kilonovae into rate limits in Section 5. We summarize our conclusions and future outlook in Section 6.

2. ZTFReST

A solid identification of rare transients such as kilonovae and orphan afterglows require multiband, and often, multiwavelength or multi-messenger data. To make this possible, one must first determine which of the many transients identified could be objects of interest based on their magnitude and color evolution, among other parameters. Once a strong candidate has been identified, the goal is to perform spectroscopic classification, when possible, and build a well-sampled, multiwavelength light curve to characterize the system. This is particularly interesting for kilonovae as photometry and spectroscopy make it possible to extract information about the ejecta and therefore the original progenitor system (e.g., Coughlin et al. 2018). Given the overall interest in kilonovae, coupled with their observational properties, it is important to prioritize rapidly fading and/or reddening candidates with no history of variability.

ZTFReST relies on the ZTF alert stream (Patterson et al. 2018), which reports information about all 5σ detections, including its magnitude, proximity to other sources and its previous history of detections, among other metrics; it uses the alert stream from both public and private surveys (Bellm et al. 2019). The largest public survey during ZTF Phase I had a three-night cadence, while ZTF Phase II predominantly has a two-night cadence. The public surveys in both ZTF Phase I and II obtain one 30 s exposure in both the g band and r band every night a field was observed. The largest private program has been an extragalactic transient survey with a 1 day cadence, where g- and r-band exposures are obtained six times per night; this survey covers $\approx$3000 deg^2 at high Galactic latitude ($\sim|b_{\mathrm{Gal}}| > 30°$). The ZTF partnership has also conducted a wide i-band survey that supplements this survey.

The flowchart in Figure 1 offers a visual summary of ZTFReST, which is publicly developed on GitHub.[23] Much of the infrastructure is built upon the pipeline described in Andreoni et al. (2020b) for historical, serendipitous kilonovae searches. Here we describe the set of procedures that streamline the pipeline in order to perform near real-time searches.

2.1. Alert Stream Database Queries

The alerts from both public and private surveys are queried using a local instance of Kowalski,[24] an open-source, multi-survey data archive and alert broker (Duev et al. 2019). In addition to storing all ZTF alert/light-curve data in a single MongoDB, Kowalski also has built-in capabilities of matching against external catalogs. We regularly query Kowalski to identify the transients that pass specific criteria. In particular, we are interested in transients that are (i) astrophysical in nature, i.e., unlikely instrumental artifacts; (ii) short lived; (iii) without previous history of variability; and (iv) without a spatially coincident stellar counterpart. Appropriate queries to Kowalski can address these requirements. The real/bogus score drb, which is used to ensure transients are astrophysical in nature, is based on a deep learning classification algorithm (Duev et al. 2019). We employ a threshold of drb > 0.9, for which Duev et al. 2019 measured a false positive rate of 0.4% at the cost of a false negative rate of 5%. For further details regarding the other query parameters, we refer the reader to Andreoni et al. (2020b).

2.2. Light-curve Generation and Fitting

The main focus of this pipeline is to find transients undergoing rapid luminosity evolution, and in particular, those that are rapidly fading. Therefore, we take a set of light curves for each transient and fit them to a linear model in magnitude space, to measure either the decay or rise rates, in units of magnitudes per day. This metric has been used in the past (Kasliwal et al. 2020) to model the luminosity evolution of kilonovae, and provides a straightforward approximation for the luminosity evolution over the timescales and passbands we are interested in here. For each candidate, up to three types of light curves can be generated: a light curve based on the content of the ZTF alerts, a PSF forced-photometry light curve, and a nightly *stacked* light curve, built by combining forced-photometry measurements (see below).

The light curves from the alerts are compiled with the full candidate detection history (the prv field in the alert packets), thus including $3 \leqslant S/N \leqslant 5$ detections found by the ZTF pipeline prior to the initial $>5\sigma$ alert. First, we make a cut on the observed duration, both filter agnostic and per band. We select only candidates with a maximum total duration of 14 days (i.e., reject any candidates whose difference between first and last detection exceeds 14 days) and a maximum single-band duration of 10 days, 12 days, and 14 days in the g, r, and i bands respectively; these numbers were broadly tailored to a conservative estimate of kilonova fade rates and expected ZTF limits for kilonovae in the local universe based on POSSIS-based (Bulla 2019) grid of kilonova models spanning the plausible binary neutron star parameter space (Dietrich et al. 2020). Second, we perform linear fits in magnitude versus time space when light curves have multiple detections over at least a 0.5 day baseline in a given band. As part of the initial filtering criteria, the fits are not weighted and no chi-squared metric or similar is evaluated; candidates that pass these criteria are subject to more detailed fits accounting for this, described below. We place a hard constraint of fading at least 0.3 mag day^{-1} in any one of the g, r, or i bands, as shown to be appropriate for a wide-range of kilonova model grids
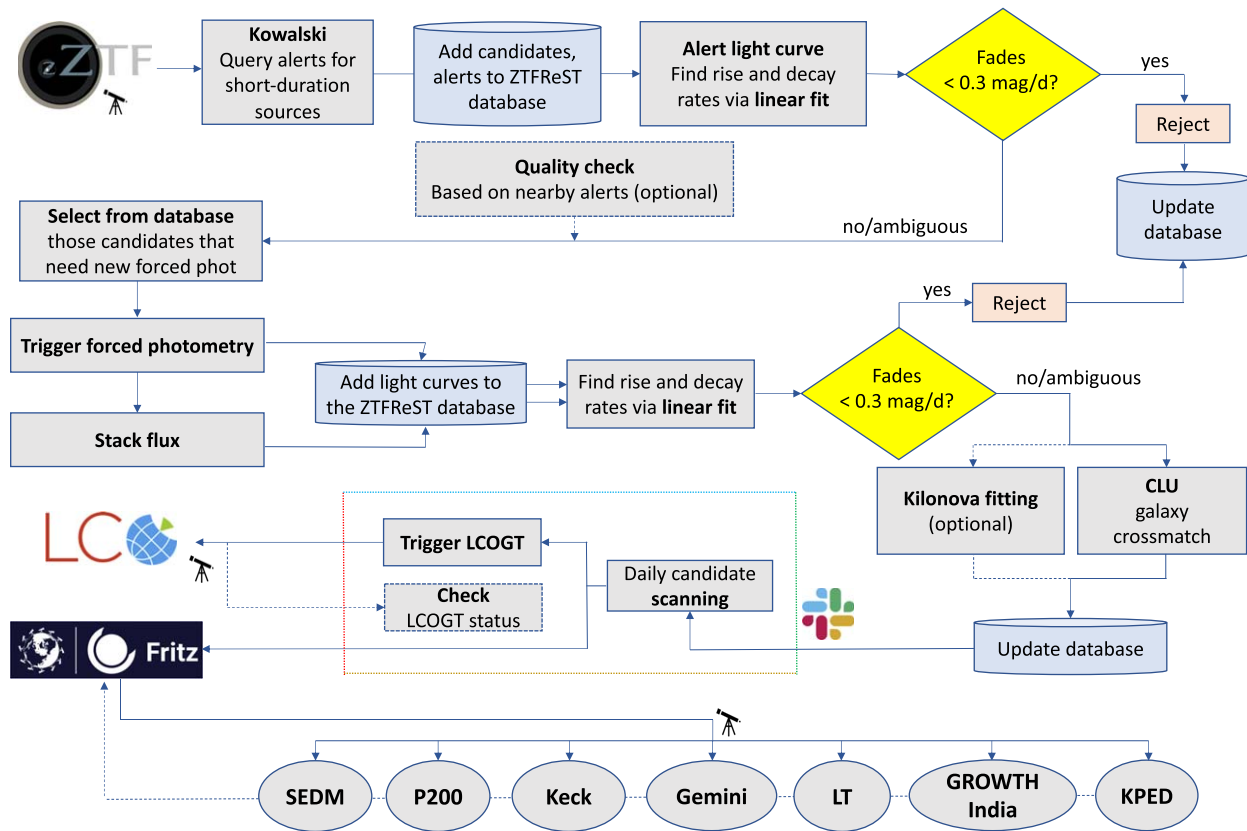

Figure 1. ZTFReST flowchart. Alerts are queried using Kowalski and their light curves undergo a first selection, where slow-evolving transients with observed long durations are rejected. Then, a second selection is performed on PSF forced photometry and nightly-binned *stacked* photometry. During daily scanning using the Slack application, transients are prioritized based on their fade rate and possible association with nearby galaxies present in the CLU catalog. Follow-up photometry with LCO telescopes is automatically triggered for kilonova candidates directly from Slack. Finally, LCO data are downloaded and processed with an external image-subtraction and forced-photometry pipeline. The most interesting candidates, along with LCO photometry results, are then uploaded to the ZTF Phase II marshal, known as Fritz.

(Andreoni et al. 2020e; Kasliwal et al. 2020). Those candidates that do not pass this threshold are rejected from further consideration.

For those objects which are either fading faster than this threshold or for which there is not currently enough signal to noise in the existing observations to tell, we perform a data quality check based on nearby alerts. If there were recent alerts within 3″ of the object and different ID (i.e., further than 1″), it is possible that the candidates are artifacts caused by electronic crosstalk or by reflections within the optical system (known as *ghosts*). For those objects not rejected by this criteria, PSF photometry is performed pinned to the median location of each candidates' set of alerts using ForcePhotZTF (Yao et al. 2019), on images processed with the ZTF pipeline at IPAC (Masci et al. 2019) using the ZOGY image-subtraction algorithm (Zackay et al. 2016). The precise coordinates of the candidates are obtained from the median location reported in the ZTF alerts.

At this point, we created *stacked* light curves, where the forced-photometry flux within each night in each band is *optimally* combined. Specifically, we use a weighted average when all the data points have $S/N \geqslant 3$, where the squares of the S/N are used as weights. If a night includes at least one data point with $S/N < 3$, a simple mean is used. Numerous tests revealed that stacking flux this way reduces significantly the number of spurious low-S/N detections, while providing us with deeper and more precise photometry of sources with

$S/N < 3$ in individual exposures (see Figure 2 in Andreoni et al. 2020e).

The fit to linear models is repeated for both the forced and stacked photometry. Only significant data points with $S/N \geqslant 3$ are considered for the fit. Once again, candidates failing the observed duration constraints (see above) and the 0.3 mag day^{-1} cut are rejected from further consideration if their light curves have sufficient signal to noise and baseline to fit to linear models.

2.3. Galaxy Catalog Crossmatching

Those objects that pass the 0.3 mag day^{-1} cut are cross-matched with galaxies further than 10 Mpc in the Census of the Local Universe (CLU) catalog (Cook et al. 2019), with a *match* declared if the catalog-reported location of the galaxy is within 100 kpc of the transient's location (Berger 2014); this catalog is especially useful given its completeness (85% in star formation and 70% in stellar mass at 200 Mpc). Catalogs like CLU and Galaxy List for the Advanced Detector Era (GLADE; Dálya et al. 2018) have proven to be very useful for galaxy-targeted follow-ups of gravitational-wave events, including GW170817 (Arcavi et al. 2017; Coulter et al. 2017; Valenti et al. 2017), especially powerful given it reduces the sky area requiring covering to ≈1% within these local volumes out to ∼200 Mpc (Cook et al. 2019). Given the intrinsically faint absolute magnitudes of kilonovae, the presence of a transient in a known nearby galaxy could make it particularly interesting. Even if

there is no match, we include the candidate in the scanning step, i.e., this is a value-added diagnostic.

2.4. Kilonova Model Fitting

At this point, we have two optional features implemented. The first employs automated fits to kilonova light-curve model grids, such as those provided by Kasen et al. (2017) and Bulla (2019), combined with a Gaussian process regression framework (Coughlin et al. 2018, 2019a; Dietrich et al. 2020). In particular, due to the limited number of light-curve points, we reduce dimensionality with single component light-curve models by default; however, multiple component models with both *dynamical ejecta* and disk winds driven by neutrino energy, magnetic fields, viscous evolution and/or nuclear recombination are also available (e.g., Metzger et al. 2008; Bauswein et al. 2013; Dietrich & Ujevic 2017; Siegel & Metzger 2017). Unlike fitting to GW170817 or similar, neither the explosion time nor the distance is fixed, and therefore in addition to the model parameters such as the ejecta masses, ejecta velocities, lanthanide fractions, inclination angles, among others, both the distance modulus and the explosion time must be fit for. For now, we optionally perform the fits; in the future, we desire to use these fits to prioritize follow-up resources and use the fit efficacy to assign a probability of *discovery*.

2.5. Semiautomatic Follow-up Triggering

The second feature is to automatically trigger follow-up observations based on the LCO network (Street et al. 2018). The ZTF survey cadence may be insufficient, on its own, to fully characterize the fast decaying light curves of afterglows and kilonovae, especially when considering loss of time due to weather or bright moon phases; in general, both the inclusion of *i*-band exposures as well as three epochs per night in 3–5 night blocks can lead to high detection efficiencies (Almualla et al. 2021). For this reason, automated infrastructure to trigger on particularly interesting candidates has been implemented.

The objects surviving the selection criteria are scanned by on-duty astronomers within dedicated `Slack` application channels built for this purpose. The astronomers' role is to vet automatically selected candidates to separate likely extragalactic fast transients from other sources such as bogus detections, stellar flares, or slowly evolving transients that were not rejected automatically due to outliers in their light curve. We use a set of scores, built based on the presence of rapid decay, proximity to a CLU galaxy, distance from the Galactic plane, and others in order to prioritize the candidates for scanning; we do not make any cuts on ecliptic latitude. Within the `Slack` channel, textual information such as the coordinates, fade rates, CLU galaxy crossmatch, Galactic latitude, and expected extinction are listed. We also display both the discovery, reference, and difference images, as well as the photometric time series plotted separately for the alert, forced photometry, and stacked photometry data streams. From within `Slack`, we can trigger LCO network (Street et al. 2018) observations directly with a simple command. These data obtained with LCO are reduced automatically using a dedicated pipeline (Fremling et al. 2016) and uploaded in the Global Relay of Observatories Watching Transients Happen (GROWTH) marshal (Kasliwal et al. 2019a) during ZTF Phase I and in the Fritz marshal (Duev et al. 2019; van der Walt et al. 2019) during ZTF

Phase II; these marshals are used for examining all relevant proprietary and external data sets rapidly, enabling communication between collaboration members and triggering further follow-up observations of interesting objects.

3. Science Validation and First Results

Since 2020 September 21, we have been running `ZTFReST` every day. We validated the output of the pipeline by running it first on 265 days of ZTF *archival* data, from 2020 January 1 to 2020 September 20, and blindly scanning for candidates; from then on, new data was processed daily. On ∼7% of nights, the dome is closed and there is no new data; a further ∼3% of nights have poor conditions such that the magnitude limits are 2 magnitudes brighter than the median limits for the survey. A summary of the confirmed extragalactic fast transients (along with one yet unclassified source) identified during science validation can be found in Table 1.

3.1. Science Validation I: Archival Data

The `ZTFReST` code allows us to easily input a range of dates to search for candidates, with the default being the last 24 hr from the time when the pipeline starts running.

The 265 days of data used for the science validation yielded 81,651,645 alerts in total. We identified 15,555 short-duration (at most 14 days between the first and last detection) transient candidates using `Kowalski`. Since the main objective of this science validation is to understand the `ZTFReST` capability to find extragalactic fast transients, we limited our queries to high Galactic latitudes by imposing a $|b_{Gal}| > 10°$ cut, which brings the number of candidates to 12,710. The candidates with a fading rate faster than $0.3 \, \mathrm{mag \, day^{-1}}$ in at least one band with at least one photometry method (alerts, forced photometry, or stacked forced photometry) are 309. Of these candidates, we reject 132, as they have a slow evolution (fade rate slower than $0.3 \, \mathrm{mag \, day^{-1}}$) in at least one band; while this requirement is not used for our real-time processing (see below), it was useful to limit the number of science validation candidates. This brings the number of candidates down to 177, of which 29 are located within 100 kpc from CLU catalog galaxies further than 10 Mpc. To demonstrate the benefit of the Galactic latitude cut in particular, Figure 2 shows the cumulative distribution of $|b_{Gal}|$ for those transients passing the criteria of fading faster than $0.3 \, \mathrm{mag \, day^{-1}}$ in at least one band; unsurprisingly, ∼45% of such transients are located $|b_{Gal}| \leqslant 10$; because there are so many stars near to the Galactic plane, the likelihood of identifying flaring stars there is very high, indicating the utility of such a cut to decrease the background of Galactic stars.

For science validation purposes, we applied criteria for light-curve evolution based on kilonova models as in Andreoni et al. (2020b). Thus, we selected those sources with fading rates larger (i.e., faster) than $0.57 \, \mathrm{mag \, day^{-1}}$ in the g band, $0.39 \, \mathrm{mag \, day^{-1}}$ in the r band, or $0.3 \, \mathrm{mag \, day^{-1}}$ in the i band; again, this is a stricter cut than used in our real-time processing (see below). Only 40 candidates passed the strict selection criteria. We vetted the candidates by inspecting, for each one of them, small cutouts of the science image, the reference image, and the image subtraction, the light curve built with information included in the ZTF alerts, the forced PSF photometry light curve, and the nightly stacked PSF photometry light curve. Twelve candidates found during archival searches passed human inspection that were not already

Table 1

Afterglows Found with ZTFReST During Science Validation, in Both Archival Searches (Above the Horizontal Line; Section 3.1) and in Real-Time (Below the Horizontal Line; Section 3.2)

Name	TNS	RA	Dec	b_{gal} (deg)	Classification or GRB	z	Ref.	Fade g (mag/d)	Fade r (mag/d)
ZTF20aajnksq	AT2020blt	12:47:04.87	+45:12:02.25	71.9	Afterglow no GRB	2.9	[1]	⋯	1.58
ZTF20abbiixp	AT2020kym	14:12:10.34	+60:54:19.01	53.6	GRB200524A	1.256	[2]	⋯	3.07
ZTF20abwysqy	AT2020scz	00:27:08.55	+34:01:38.36	−28.6	GRB200826A	0.71	[3]	2.01	⋯
ZTF20abtxwfx	AT2020sev	16:41:21.23	+57:08:20.67	40.0	GRB200817A	⋯	TW; [4]	0.49	0.48
ZTF20acgigfo	AT2020urd	00:40:31.10	+40:35:53.90	−22.2	Nova	⋯	TW	⋯	0.62
ZTF20acstbfh	AT2020aapw	00:40:19.74	+40:49:35.82	−22.0	Nova	⋯	TW; [5]	0.61	⋯
ZTF20acozryr	AT2020yxz	02:48:44.33	+12:08:14.16	−41.5	GRB201103B	1.105	TW; [6]	0.75	0.78
ZTF21aaarlbp	AT2021bl	01:33:21.99	+30:33:01.27	−31.5	Nova	⋯	TW	0.81	0.87
ZTF21aabxjqr	SN2021pb	09:44:46.80	+51:41:14.41	47.4	Shock cooling	0.033	TW; [7, 8]	0.40	0.28
ZTF21aaeyldq	AT2021any	08:15:15.34	−05:52:01.23	15.7	Afterglow no GRB	2.514	[9]	⋯	17.56
ZTF21aagwbjr	AT2021buv	07:48:19.30	+11:24:34.32	17.7	GRB210204A	0.876	TW; [10]	⋯	2.34
ZTF21aahifke	AT2021clk	02:54:27.54	+36:31:56.74	−20.1	Unknown	⋯	TW; [11]	⋯	0.96
ZTF21aapkbav	AT2021gca	14:28:07.33	+33:29:49.38	68.2	Shock cooling	0.036	TW; [7, 12]	0.29	0.31

Note. The names of the three new, confirmed afterglows discovered by ZTFReST are marked in boldface. For each transient, this table presents its Transient Name Server (TNS) denomination, coordinates (J2000), Galactic latitude, classification, or associated GRB when known, discovery references, and fade rate at the time of discovery in the g and r bands. In particular, the highest fade rates measured using ZTF alerts, forced photometry, and nightly stacked forced photometry are reported.
References: TW (this work); [1] Ho et al. (2020c); [2] Ho et al. (2020b); [3] Ahumada et al. (2020); [4] Andreoni et al. (2020d); [5] Taguchi et al. (2020); [6] Coughlin et al. (2020c); [7] U. C. Fremling et al. 2021, in preparation; [8] Milisavljevic et al. (2021) [9] Ho et al. (2021); [10] Kool et al. (2021); [11] Andreoni et al. (2021a); [12] Andreoni et al. (2021b).
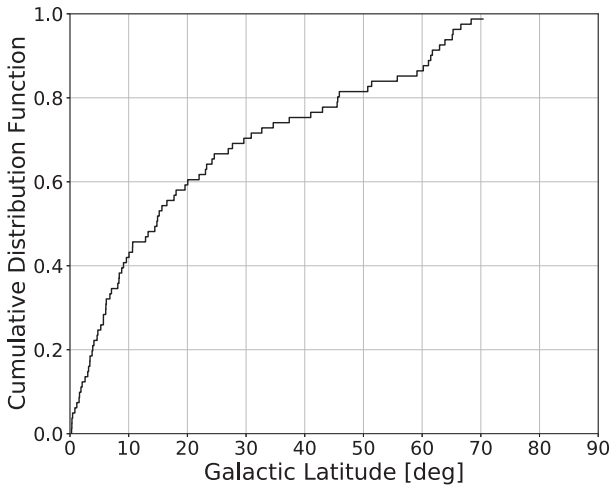

Figure 2. Cumulative distribution of $|b_{Gal}|$ for those transients passing the criteria of fading faster than 0.3 mag day^{-1} in at least one band.

classified as cataclysmic variables (CVs). Of those, eight were excluded from the sample after further vetting. In particular, for one candidate, faint detections were revealed by forced photometry on every ZTF image available; three showed multiple outbursts in ATLAS, found using the forced-photometry server (Tonry et al. 2018; Smith et al. 2020); one had an underlying point source classified as "PSF" by Legacy Survey DR9 (Dey et al. 2019) tractor modeling; one appears to be a very slow moving object. Two are located at Galactic latitude $10 < |b_{Gal}| < 15$ deg in crowded stellar fields, appear to be hostless, and show blue or *gray* color ($g - r \leqslant 0$ mag), which suggests that they are more likely stellar outbursts rather than cosmological afterglows, kilonovae, or other types of genuine extragalactic transients.

Four sources passed all of our tests and are either confirmed or likely GRB afterglows:

1. ZTF20aajnksq (AT2020blt) was spectroscopically classified as an afterglow at redshift $z = 2.9$, with no associated gamma-ray counterpart (Ho et al. 2020c).
2. ZTF20abbiixp (AT2020kym) was likely the optical counterpart to GRB 200524A, already found serendipitously in ZTF data by Ho et al. (2020b). Optical spectroscopy suggests that the most probable redshift is $z = 1.256$ (Yao et al. 2021). This object will be discussed in a paper in preparation on afterglows discovered in ZTF (Q. Y. Ho et al. 2021, in preparation).
3. ZTF20abwysqy (AT2020scz) was the confirmed optical counterpart to the short-duration GRB 200826A. This transient was found during rapid-response follow-up of a coarsely localized Fermi trigger with ZTF (Ahumada et al. 2020); it is described in detail by Ahumada et al. (2021). Follow-up observations placed it at redshift $z = 0.7481 \pm 0.0003$ (Rothberg et al. 2020).
4. ZTF20abtxwfx (AT2020sev) was not spectroscopically confirmed, but its fast-evolving light curve (Figure 3), the presence of a radio counterpart, and a possible association with GRB 200817A (Fermi GBM Team 2020) suggest it being an afterglow as well (Andreoni et al. 2020d). The multiwavelength analysis of this transient is presented in Section 4.1, and photometry is available as data behind the figure.

For a tabular summary of this discussion, please see Table 2. In addition, we ran the pipeline on data from 2019, appropriately choosing time spans of ± 7 days centered on the first detection of two known sources of interest. The former, ZTF19aabgebm (AT2019aacx), is the afterglow counterpart to GRB 190106A. The latter, ZTF19aanhtzz (AT2019aacu) is a
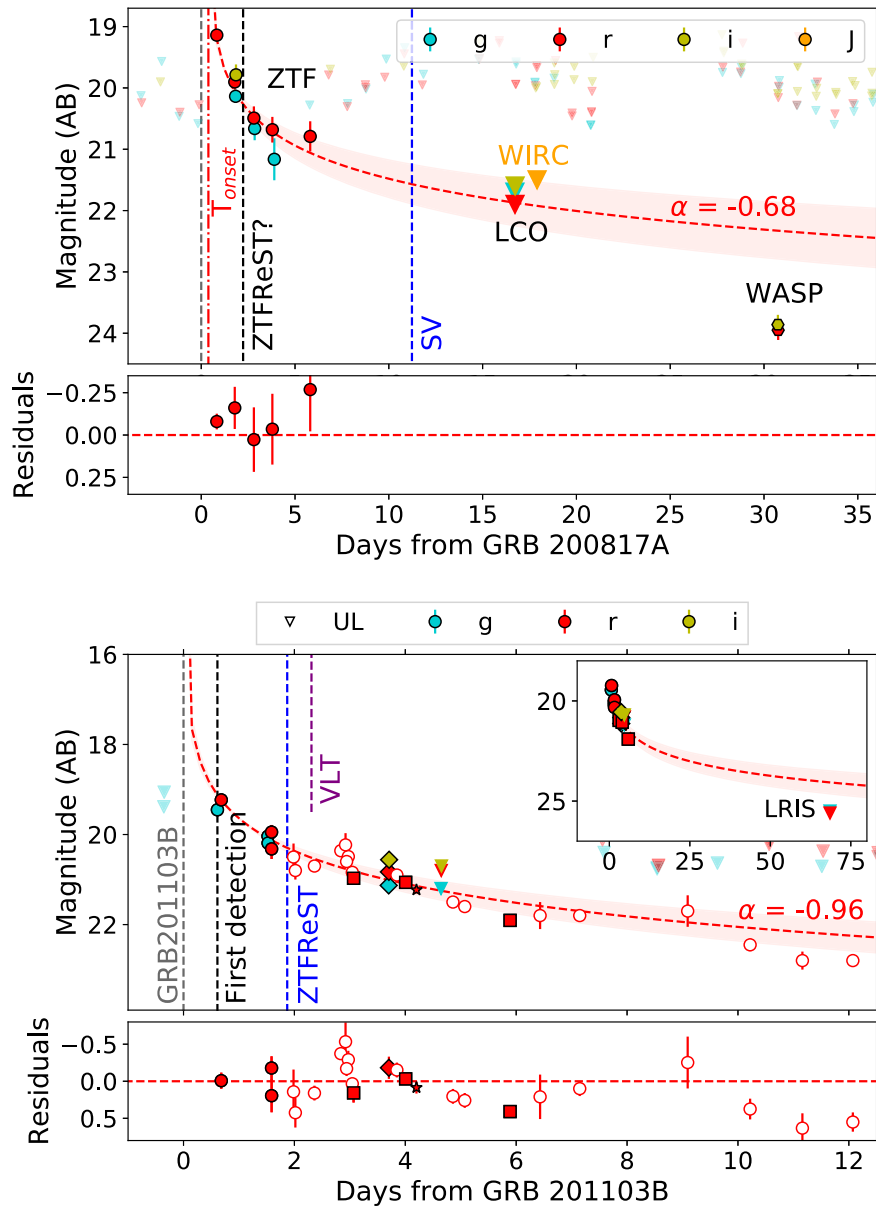
Figure 3. Forced PSF photometry light curve of the fast transients ZTF20abtxwfx (top panel) and ZTF20acozryr (bottom panel). Top row: In addition to ZTF optical data, the upper plot shows a *J*-band near-infrared (NIR) upper limit (marked by triangles for all instruments) obtained with P200+WIRC and late-time optical imaging obtained with LCO and P200+WaSP (hexagons). The abscissa is centered on the detection time of GRB 200817A, under the assumption that it is the gamma-ray counterpart to ZTF20abtxwfx. The onset time estimated from the power-law fit, T_{onset}, is indicated by a vertical red line; the shaded region indicates the 1σ uncertainty on the power-law index; the fit residuals are shown in the bottom panel. The times of discovery during science validation (SV), the expected near real-time discovery time (during regular `ZTFReST` operations), and the GRB 201103B trigger time are indicated by vertical dashed lines. Fit residuals are shown for all *r*-band data points in the lower panel. Bottom row: In addition to ZTF optical data (solid circles), the upper plot shows our LCO (diamonds), LT (stars), and GIT (squares) follow-up observations. Open circles mark data points published by other groups via Gamma-ray Coordination Network (GCN) circulars in the *r* or *R* bands. The abscissa is centered on the detection time of GRB 201103B. A power-law fit was performed using only ZTF, LCO, LT, and GIT *r*-band data for a fixed onset time, equal to the discovery time of GRB 201103B. Fit residuals are shown for all *r*-band data points in the lower panel. The near real-time discovery time of ZTF20acozryr is indicated with a blue dashed line. The purple dashed line marks the time when ZTF20acozryr was spectroscopically classified using X-Shooter on VLT (Xu et al. 2020).

(The data used to create this figure are available.)

transient found at high Galactic latitude ($b_{Gal} = 59°$) that faded by $\Delta r = 1.24$ mag day^{-1} (Andreoni et al. 2020e). Both ZTF19aabgebm and ZTF19aanhtzz were successfully recovered.

3.2. Science Validation II: Real-time Operations

Daily data processing with `ZTFReST` started on 2020 September 21. Every morning at 07:30 AM Pacific Time, when all the images acquired during the night are processed

by the image-subtraction pipeline at IPAC (Masci et al. 2019), a `crontab` automatically starts `ZTFReST`. After ∼30 minutes, `ZTFReST` finishes all the operations and a bot announces to the team that the analysis is complete via the `Slack` application (see also Section 2.5). While this process is currently run once per night, we may explore running halfway through the night to potentially identify some fast transients earlier in the future, possible due to the participation by scientists worldwide.

Table 2
Filtering Results for ZTFReST on 265 Days of Archival Science
Validation Data

Filtering Criteria	# of Cand.	Norm. (deg^{-2} y^{-1})
Science validation	15,555	2.5630
$|b_{\mathrm{Gal}}| > 10°$	12,710	2.7478
At least one band: 0.3 mag day^{-1}	309	0.0668
All bands: 0.3 mag day^{-1}	177	0.0383
Kilonova-like fade rates	40	0.0086
Not previously identified CVs	12	0.0026
Likely afterglows	4	0.0009
Likely kilonovae	0	0

Note. We show the number of transients that pass each step, having applied that criteria over the remaining transients from the previous stage. The criteria are further described in Section 3.1. The number of candidates that pass each step is also reported normalized per square degree and unit of time, considering an average coverage of 9889 deg^2 (7537 deg^2 at $|b_{\mathrm{Gal}}| > 10°$) per night and 224 nights in which data were successfully taken.

In the first ∼4 months of operations, the pipeline has yielded between 0 and 11 candidates per day by requiring a conservative fading rate larger than 0.3 mag day^{-1}. This threshold is less restrictive than those thresholds used for archival searches, tailored for fully evolved kilonovae, which mitigates the risk of missing fast transients close to peak. The median and mean number of candidates to be scanned per day has been 2 and 2.5, respectively, with a standard deviation of 2.4 candidates per day. Similarly, there have been a mean of 0.5 new candidates per day, with a peak of 5. No cut on the Galactic latitude has been applied.

Among the large number of sources found in near real time, the transients we identified as extragalactic fast transients were:

1. ZTF20acgigfo (AT2020urd) and ZTF20acstbfh (AT2020aapw)—Novae in the M31 galaxy.
2. ZTF20acozryr (AT2020yxz)—Spectroscopically confirmed afterglow of long GRB 201103B. ZTF20acozryr is described in detail as a case study in Section 4.2.
3. ZTF21aaarlbp (AT2021bl)—Nova in the M33 galaxy.
4. ZTF21aabxjqr (SN2021pb)—Shock cooling of a Type IIb supernova at redshift $z = 0.033$ (U. C. Fremling et al. 2021, in preparation).
5. ZTF21aaeyldq (AT2021any)—Afterglow discovered serendipitously in ZTF data (Ho et al. 2021) without any associated GRB. Spectroscopic observations allowed a redshift of $z = 2.514$ to be measured and confirmed the nature of the transient (de Ugarte Postigo et al. 2021). ZTF21aaeyldq was discovered as part of the high-cadence partnership survey by a filter designed to find fast transients described in (Ho et al. 2020c; Perley et al. 2021). The transient was missed during ZTFReST real-time operations because the time difference between the first and last detection in ZTF data was lower than our minimum baseline for light-curve fitting of 0.5 days. Since the identification of ZTF21aaeyldq on 2021 January 16, we changed the threshold from 0.5 days to 0.125 days (3 hr). This allowed us to correctly recover ZTF21aaeyldq, which will be discussed in detail in future work (Q. Y. Ho et al. 2021, in preparation).
6. ZTF21aagwbjr (AT2021buv)—Confirmed afterglow of GRB 210204A (Kool et al. 2021; Hurley et al. 2021) at
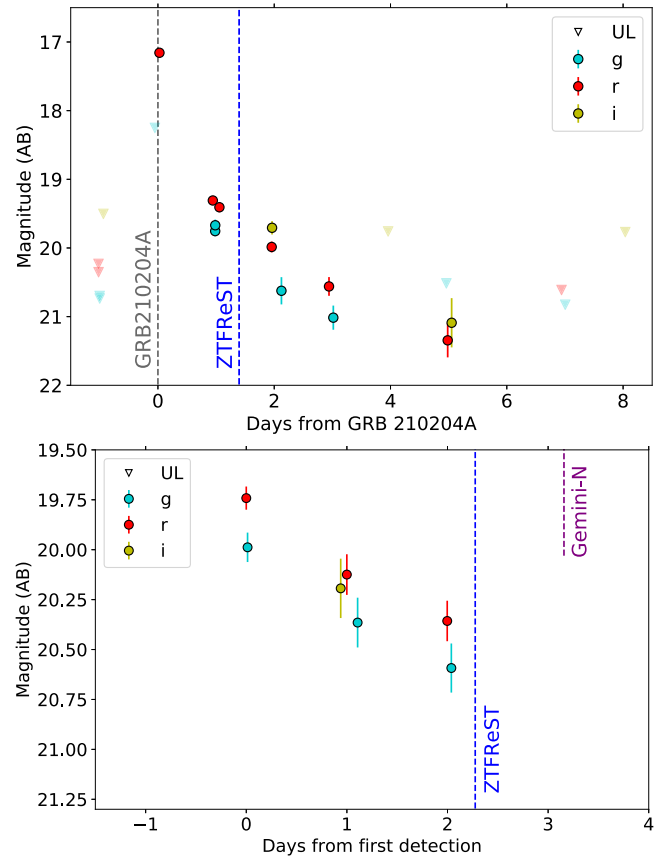

Figure 4. Photometric light curves of the fast transients ZTF21aagwbjr (top), the optically discovered afterglow of GRB 210204A, and Type II supernova ZTF21aapkbav (bottom).

(The data used to create this figure are available.)

redshift $z = 0.876$ (Xu et al. 2021). ZTF photometry constrained the explosion time within 1.9 hr from the first detection. The transient was independently discovered also by the fast-transient filter described in Ho et al. (2020c). The light curve of ZTF21aagwbjr is shown in Figure 4; the photometry is available as data behind the figure. A dedicated work presenting multiwavelength analysis of this source is planned (H. Kumar et al. 2021, in preparation).

7. ZTF21aahifke (AT2021clk)—Fast transient found in ZTF data (Andreoni et al. 2021a) and rapidly confirmed with the GROWTH-India Telescope (GIT) follow-up observations. The nature of ZTF21aahifke, whose analysis is presented in Section 4.3, is still unknown.
8. ZTF21aapkbav (AT2021gca)—Fast transient discovered on 2021 March 19 (Andreoni et al. 2021b) associated with the nearby galaxy GALEXMSC J142807.45+332950.0 at redshift $z = 0.036$ (Kochanek et al. 2012), as tabulated by the NASA/IPAC Extragalactic Database (NED). Under the assumption that ZTF21aapkbav and the galaxy are associated, the absolute magnitude of the transient's first (and brightest) detection was $M_r = -16.33 \pm 0.06$ mag. The fade rate of 0.3 mag day^{-1} that we measured from ZTF photometry (Figure 4, photometry available as data behind the figure) in both the g and r bands was confirmed by follow-up with the Lulin One-meter Telescope as part of the Kinder survey (Chen et al. 2021). The last ZTF upper limit

before the first detection was measured on 2021 March 08 at 06:27 UT, which constrains the onset time to be within <9.1 days from the first detection. Our team promptly triggered spectroscopy with Gemini North telescope equipped with the Gemini Multi-Object Spectrograph instrument.[25] The spectrum revealed a broad Hα feature extending to velocity $v \sim 9000$ km s^{-1} and possibly He I ($\lambda = 5876$). The redshift was coarsely measured and consistent with the NED tabulated value. We concluded that ZTF21aapkbav was a fast-evolving supernova of Type IIb (see also U. C. Fremling et al. 2021, in preparation).

4. Case Studies

In this section, we present three case studies. Two are new, confirmed afterglows discovered by ZTFReST, namely, ZTF20abtxwfx (AT2020sev) and ZTF20acozryr (AT2020yxz). The discovery process and GRB association will be described, along with multiwavelength follow-up and data analysis. The third case study is a fast transient of unknown origin, ZTF21aahifke (AT2021clk).

4.1. ZTF20abtxwfx

The discovery of ZTF20abtxwfx (AT2020sev) occurred during science validation on 2020 August 28, which is about 10 days after the first detection in ZTF data, when ZTFReST was not yet being used in real time. During present operations, a transient like ZTF20abtxwfx would be deemed worthy of spectroscopic and photometric follow-up after the second night post-discovery (Figure 3).

Multiwavelength follow-up revealed a radio counterpart to ZTF20abtxwfx (Nayana & Chandra 2020), which suggests the transient to be a cosmological afterglow. Specifically, it is possible that ZTF20abtxwfx is the optical counterpart to GRB 200817A (Fermi GBM Team 2020) or of a GRB that went undetected. Here we briefly present optical, NIR, and radio follow-up of the transient, along with gamma-ray analysis carried out in a time frame where we could expect the onset of the event to be placed (including when GRB 200817A occurred).

4.1.1. Optical and NIR

ZTF20abtxwfx was first detected on 2020 August 18 at 05:20 UT, hereafter labeled $T_{\rm det}$. The ZTF forced-photometry optical light curve (Figure 3; photometry available as data behind the figure) revealed a rapidly evolving transient that faded by ~1.3 mag in the r band in the first 2 days since $T_{\rm det}$. The transient was last detected on 2020 August 23 at 04:51 UT, at $r = 20.98 \pm 0.24$ mag. Stringent upper limits constrained the transient onset time within <1 day from $T_{\rm det}$. The color of the transient appeared to be red, with $g - r \sim 0.1$ mag and $g - i \sim 0.3$ mag one day after $T_{\rm det}$. The Galactic extinction along the line of sight was low, with $E(B - V) = 0.015$ mag (Planck Collaboration et al. 2014).

We observed the source in the NIR with Palomar 200 inch (P200) telescope equipped with the Wide Field Infrared Camera (WIRC) on 2020 September 04 at 07:06 UT. The data were reduced using the automated pipeline described in (De et al. 2020b). No source was detected at the transient

location, with 15 minutes of total exposure time, down to $J > 21.5$ (5σ). Optical follow-up observations were obtained with the LCO + 1 m Sinistro imager[26] and with P200 equipped with the Wafer-Scale Imager for Prime (WaSP).[27]

A power-law fit of the ZTF r-band light curve, converted to flux and using the expression $f = f_0 (T - T_0)^\alpha$, returned an index $\alpha = -0.68 \pm 0.124$ and an estimated onset time $T_{\rm onset}$ corresponding to 2020 August 17, 18:34:32 UT with a 1σ uncertainty of 4.08 hr (Shenoy et al. 2020a). This value of α is within 2σ of the mean of the α-value distribution presented by Del Vecchio et al. (2016). Deep optical follow-up observations performed with P200+WaSP on 2020 September 17 at 03:12 UT, reduced with the pipeline described in De et al. (2020b), significantly deviated from the power-law fit ($\sim3\sigma$), which suggests that a jet break occurred. This is evidence that, if ZTF20abtxwfx was the afterglow of a GRB, the GRB must have been on-axis, thus more easily detectable by space-based observatories than a GRB seen off-axis.

With a Bayesian analysis (P. T. H. Pang et al. 2021, in preparation) on the data with a light-curve model of a GRB afterglow (Ryan et al. 2020), kilonova (Dietrich et al. 2020) and the combination of both, the evidence for these three hypotheses are estimated. The Bayes factors for GRB afterglow against the combination of GRB afterglow and kilonova is found to be $\sim 10^{3.42 \pm 0.08}$. And the Bayes factor for GRB afterglow against kilonova is $\sim 10^{3.58 \pm 0.08}$. Both suggest a strong preference for a GRB afterglow from the optical/NIR data alone, mainly due to the r-band detection at ~5 days.

4.1.2. Radio

Radio follow-up observations of ZTF20abtxwfx were performed using the Very Large Array (VLA). We observed the field in the X band (central frequency 10 GHz) twice, on 2020 August 31 and on 2020 September 15. Data were calibrated using the automated pipeline available in the Common Astronomy Software Applications (CASA; McMullin et al. 2007), with additional flagging performed manually, and imaged using the CLEAN algorithm (Högbom 1974). On the first epoch, we found a point source spatially consistent with ZTF20abtxwfx. The flux density of the radio source was 50 μJy, with an image rms of 4 μJy in 24 minutes of on-source time (Ho et al. 2020a). On the second epoch, acquired 15 days later, the flux density of the source decreased to ~25 μJy.

A tentative detection with the upgraded Giant Metrewave Radio Telescope (uGMRT) was reported (Nayana & Chandra 2020) at central frequency 1250 MHz. Nayana & Chandra (2020) measured a flux density of 96 ± 22 μJy on 2020 September 09 UT and 78 ± 18 μJy on 2020 September 20 UT.

The presence of a fading radio counterpart supports the scenario in which ZTF20abtxwfx is the optical afterglow of a relativistic explosion. The measured decline of the radio light curve is consistent with what is commonly observed during GRB follow-up observations (e.g., Chandra & Frail 2012).

4.1.3. Gamma-Rays and X-Rays

We searched the GCN archives, the Fermi/GBM catalog, the Fermi GBM subthreshold catalog, and the *Konus-Wind* triggered and waiting mode data for any possible counterpart

---

[25] Program ID GN-2021A-Q-102, PI: Ahumada.

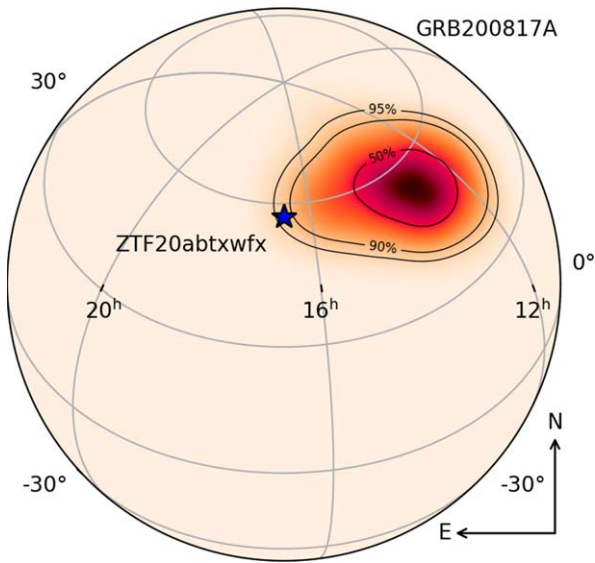[26] Programs NOAO2020B-005, PI: Coughlin; TOM2020A-008, PI: Andreoni
[27] PI: Kulkarni.

Figure 5. Fermi/GBM localization of GRB 200817A (Fermi GBM Team 2020; Goldstein et al. 2020). The optical transient ZTF20abtxwfx, marked with a blue star in the map, is included in the 93rd percentile of the localization probability. The figure was created using the `ligo.skymap` Python package.
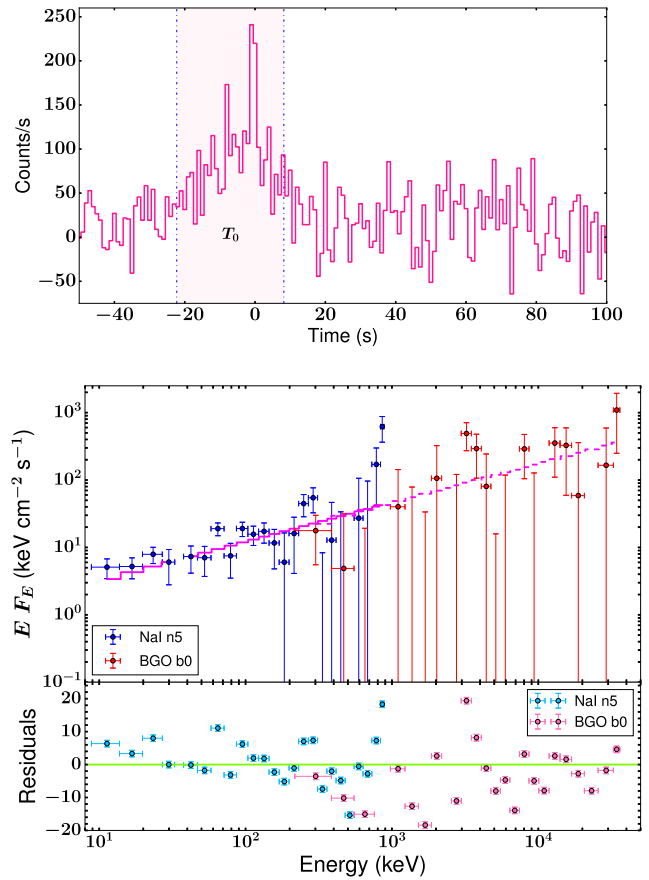

Figure 6. Fermi/GBM background subtracted light curve for GRB200817A using data from NaI detector n5 in the energy range 8–900 keV. The top panel shows the emission episodes used for the time-integrated spectral analysis covering -22.27 to 8.19 s. The bottom panel shows the broadband spectroscopy for the prompt emission episode of GRB200817A fitted with a simple power law. The blue and red data points are for NaI n5 and BGO b0 detectors, respectively.

in gamma-rays. We found one possible counterpart, GRB 200817A (Fermi GBM Team 2020). The trigger time of GRB 200817A was 2020 August 17 at 09:25:20 UT, referred to as T_0 in this section. The GRB happened in the time interval between the last optical non-detection and the first detection of ZTF and within the 3σ time interval from $T_{\rm onset}$.

ZTF20abtxwfx was located in the 93rd percentile of the Fermi localization of GRB 200817A (Figure 5; Fermi GBM Team 2020; Goldstein et al. 2020). We confirmed that the position of ZTF20abtxwfx was within the GBM field of view at the time of GRB 200817A. The initial automated classification flag identified this burst as a short GRB; however, this was due to an unusual slow rise followed by a sharp spike which resulted in an incorrect source interval selection by the automated processing. The final gamma-ray duration measure of $T_{90} = 30.46$ s results in a long GRB classification for GRB 200817A (Figure 6).

We performed a spectral analysis of GRB 200817A using Fermi/GBM data. We chose data from GBM detectors so that the boresight angle was $<50°$. For GRB 200817A, the selected detectors were n5 ($21°$) and b0 ($21°$). The GRB spectra were analyzed in a time interval of 30.46 s, equal to T_{90}, from $T_0 - 22.27$ s to $T_0 + 8.19$ s. We chose pre- and post-time intervals of 100 s for the background measurement. We have fit the data with several models including simple power law, cutoff power law, Band function, and GRBCOMP model. A simple power-law model was found to be the best-fit model, with a power-law index 1.45(±0.04) and with $E_{\rm norm}$ constrained to 100 keV (Figure 6). The model flux in the 10–1000 keV range was found to be 1.19×10^{-7} erg cm^{-2} s^{-1}.

Furthermore, we carried out a thorough search for gamma-ray counterparts to ZTF20abtxwfx in data acquired with AstroSat Cadmium Zinc Telluride Imager (CZTI). ZTF20abtxwfx was not Earth-occulted at the time of Fermi GRB 200817A as seen from AstroSat. However, when we calculated fluxes using the parameters inferred from Fermi, we concluded that it was too faint for AstroSat to detect it, since we calculated an AstroSat detection limit of $\sim3 \times 10^{-7}$ erg cm^{-2} s^{-1} for 4 s binning in the

direction of the transient. Therefore, we cannot rule out an association between ZTF20abtxwfx and GRB 200817A, despite the AstroSat non-detection.

Finally, we conducted a search for new bursts in a time window of $T_{\rm onset} \pm 12$ hr, which approximately corresponds to the 3σ time interval from the expected onset of ZTF20abtxwfx inferred from the optical light curve (see Section 4.1.1). The search did not yield any significant detection in CTZI data (Shenoy et al. 2020a). The CTZI burst closest to $T_{\rm onset}$ was GRB 200817B, which was detected on 2020 August 17 06:03:44 UT (Shenoy et al. 2020b), outside the 3σ time interval from $T_{\rm onset}$. We conclude that GRB 200817A is the most likely high-energy counterpart to ZTF20abtxwfx.

4.2. ZTF20acozryr: Serendipitous Discovery of a Long GRB Afterglow in Real Time

The optical fast-transient candidate ZTF20acozryr (AT2020yxz) was flagged by the ZTFReST pipeline on 2020 November 05 (Coughlin et al. 2020c). ZTF20acozryr was first detected by ZTF on 2020 November 03 at 09:44 UT and faded by ~0.7 mag in the g band in ~0.9 days. A g-band upper limit constrained the onset time to be within $\lesssim1$ day of the first detection. The photometry for this object is presented in Figure 3; the photometry is available as data behind the figure. The initial color of the transient appeared to

be relatively red, with $g - r \sim 0.3$ mag around the time of the first observation. The Galactic extinction on the line of sight, $E(B - V) = 0.10$ mag, was too low to be responsible for the red color.

The rapid fade rate was flagged in near real time and LCO follow-up observations were promptly triggered.[28] These observations were crucial for continued light-curve sampling for this object, given its faintness upon detection ($\sim$19.5 in the g band, $\sim$19.2 in the r band) and the measured fade rate above 0.5 mag per day. Early discovery allowed us and the community to promptly trigger follow-up observations: spectroscopy from the VLT $\sim$2.3 days later led to a measured redshift $z = 1.105$, spectroscopically confirming ZTF20acozryr to be an afterglow (Xu et al. 2020).

At the same time, a Swift ToO observation (ID 21039) was approved, resulting in a confirmation of an X–ray counterpart (Evans et al. 2020). Similarly, the IPN network confirmed consistency of the transient's location with the localization inferred for the long-duration, bright GRB 201103B (Svinkin et al. 2020) first reported by Astro-rivelatore Gamma a Immagini Leggero (AGILE; Ursi et al. 2020).

After its prompt public announcement (Coughlin et al. 2020c), ZTF20acozryr was imaged with several telescopes. Photometric follow-up was reported by Xu et al. (2020a), Zhu et al. (2020), Belkin et al. (2020b), Belkin et al. (2020a), Sharma et al. (2020), Paek et al. (2020), Belkin et al. (2020c), Belkin et al. (2020d), Volnova et al. (2020), Moskvitin & Follow-Up Team (2020), and Belkin et al. (2020e); see also Figure 3.

On 2021 January 11, about 10 weeks after GRB 201103B, we observed ZTF20acozryr with the Low Resolution Imaging Spectrometer (LRIS; Oke et al. 1995) at W. M. Keck Observatory. Data were reduced using `lpipe` (Perley 2019), a fully automatic data reduction pipeline for imaging and spectroscopy. The transient was not detected down to $r \sim g > 25.5$ mag (see the inset plot in Figure 3).

We again performed a power-law fit in the form $f = f_0 (T - T_0)^\alpha$, where T_0 was fixed to be the discovery time of GRB 201103B. For the fit, we used data acquired by our team with ZTF and during the follow-up of ZTF20acozryr with GIT, LCO, and the Liverpool Telescope (LT). The full data set can be described by a power law with index $\alpha = -1.14 \pm 0.13$. However, the low p-value of the fit ($p < 10^{-5}$) suggests that the data deviate significantly from the power-law curve. A better fit ($p \sim 0.4$) is obtained by fitting only the first 5 days after the trigger, so excluding the GIT data point taken $\sim$6 days after the GRB occurred. In this case, the data can be fit by a power law with index $\alpha = -0.96 \pm 0.06$. We suggest that a jet break occurred $\sim$4–5 days after the GRB. This scenario is consistent with reported photometry (Belkin et al. 2020a; Paek et al. 2020; Moskvitin & Follow-Up Team 2020; Belkin et al. 2020e) and with LRIS late-time data.

We perform a Bayesian analysis similar to what was done for ZTF20abtxwfx. The Bayes factors for GRB afterglow against the combination of GRB afterglow and kilonova is found to be $\sim10^{0.21 \pm 0.09}$. And the Bayes factor for GRB afterglow against kilonova is $\sim10^{1532.9 \pm 0.15}$. The extremely low evidence for the data originating from a kilonova is due to the high redshift of the detection. Again, the data suggest a GRB afterglow origin for the optical transient.

---

[28] Programs NOAO2020B-005, PI: Coughlin; TOM2020A-008, PI: Andreoni.

4.3. ZTF21aahifke: A Fast Transient of Unknown Origin

The optical fast-transient candidate ZTF21aahifke (AT2021clk) was identified as a rapidly declining source on 2021 February 7, with a fade rate of 0.96 mag day^{-1} (Andreoni et al. 2021a). The discovery of ZTF21aahifke as a fast-fading source was made possible by forced photometry on the first night after its $>5\sigma$ detection. No underlying source could be seen at the transient location in Pan-STARRS archival images down to $\sim$23 mag. Photometric follow-up with GIT confirmed the transient detection as well as the rapid decline of its brightness (Figure 7; photometry is available as data behind the figure). LCO photometry (TOM2020A-008, PI: Andreoni) in the g and i bands 4 days from the first detection placed upper limits that ruled out a significant re-brightening, or extreme optical colors, of the source. At the time of first detection, the color of ZTF21aahifke appears to be red, with $g - r \sim 0.3$ mag. The Galactic extinction on the line of sight is $E(B - V) = 0.12$ mag (Planck Collaboration et al. 2014), too low to explain the red colors.

We used forced photometry to search for previous activity in 1109 ZTF epochs taken before the 2020 February 6, without finding any significant detection. Previous activity was also searched for and not found in the Pan-STARRS (Chambers et al. 2016) Data Release 2 catalog and in ATLAS images, explored via the public forced-photometry server (Tonry et al. 2018; Smith et al. 2020). Deep Pan-STARRS images did not reveal any underlying source at the transient location. The closest source is the SDSS J025427.89+363151.5 galaxy, $\sim$6.6$''$ away from ZTF21aahifke, with Sloan Digital Sky Survey (SDSS) photometric redshift of $z = 0.433 \pm 0.1735$; at this redshift, such an offset is unlikely for afterglows. We found no Fermi or Swift gamma-ray burst alert, issued in the 22.3 hr between the last non-detection and the first detection of ZTF21aahifke, with compatible localization (95%). GIT follow-up photometry shows a steepening of the light curve (Figure 4), which could suggest the presence of a jet break, under the assumption that ZTF21aahifke is another untriggered GRB afterglow.

On 2021 February 20, one epoch of radio data was acquired with VLA (PI Perley). The data were reduced in the same way as for ZTF20abtxwfx. No radio counterpart to ZTF21aahifke was found, $\sim$15 days from the transient onset, with an rms of 7 μJy.

We also perform a Bayesian analysis similar to what was done for ZTF20abtxwfx. Leaving the distance as a free parameter, the Bayes factors for a kilonova against a GRB afterglow is found to be $\sim10^{4.37 \pm 0.08}$. And the Bayes factor for kilonova against GRB afterglow plus kilonova is $\sim10^{0.04 \pm 0.06}$. The moderate favoring for the kilonova hypothesis is due to the non-detection at 5 days, which is mildly constraining to the afterglow model best fit to the early points, and does not have a potential jet break encoded, while the kilonova model has dropped well below the limit by that time. Although ZTF21aahifke shares similarities with other afterglows observed with ZTF, we cannot confidently exclude a kilonova or a Galactic origin, such as from a cataclysmic variable and other Galactic fast transients identified in the survey (Andreoni et al. 2020e).

5. Kilonova Rate

Real-time searches for extragalactic fast transients make it possible to determine the rates of kilonovae, improving the results obtained by Andreoni et al. (2020b) and approaching
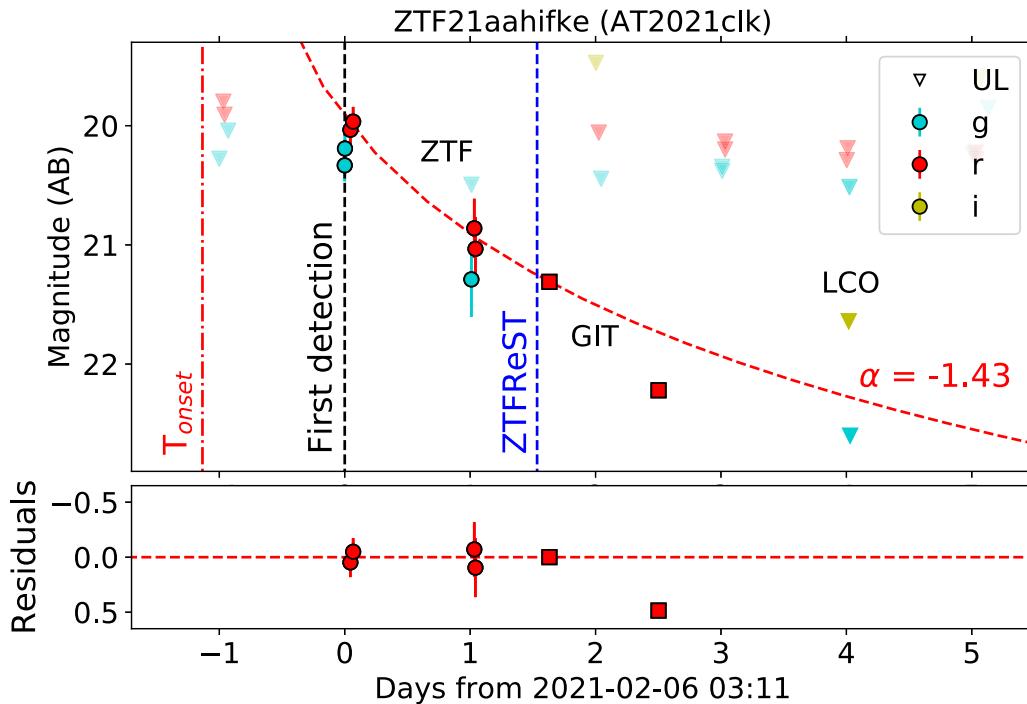
Figure 7. Photometry light curve of the fast transient ZTF21aahifke, which does not have any known associated gamma-ray counterpart. The power-law fit to the ZTF detections and the first GIT data returns results with very large uncertainties. The resulting onset time ($T_{\rm onset}$) is placed on 2021 February 4 23:57 (before the last ZTF non-detection preceding the discovery of ZTF21aahifke), with a standard deviation of 1.57 days, and the power-law index is $\alpha = -1.43 \pm 1.27$.

(The data used to create this figure are available.)

those of Kasliwal et al. (2017), and therefore the rates of binary neutron star (and neutron star−black hole) mergers.

In this work, we combined results from archival and real-time searches. During 7 months of archival searches with a cut at Galactic latitude $b_{\rm Gal} > 10°$, the number of fields explored is consistent with Andreoni et al. (2020b) within 1%. During 5 months of real-time operation, no cut in Galactic latitude was applied, thus 23% more fields were explored than in Andreoni et al. (2020b), albeit with higher Galactic extinction and in typically more crowded fields. Thus, the following results can be considered conservative.

Andreoni et al. (2020b) constrained the GW170817-like kilonova rate to be $R < 1775$ Gpc^{-3} yr^{-1} (95% confidence) with 23 months of ZTF survey data. In this paper, we have analyzed more than 12 additional months of ZTF survey data with methods more conservative than those used by Andreoni et al. (2020b); we found no confirmed kilonova.

As in Andreoni et al. (2020b), we used simsurvey (Feindt et al. 2019) to inject kilonova light curves in ZTF survey data and infer the kilonova rate by measuring the number of synthetic kilonovae recovered by the software. The new analysis ranged data spanning 2020 February 22 to 2021 March 03. To be *detected*, we required that recovered light curves have a fade rate larger than 0.3 mag in each band; in addition, we required at least two detections with $>3\sigma$ significance, at least one of which must have $>5\sigma$ significance, and >3 hours of time separation. Injected uniformly in comoving volume, the light curves follow the assumed kilonova models and are affected by redshift, reddening from Milky Way extinction and survey specifics like the limiting magnitude and cadence. The limiting magnitudes vary between 20.2 ± 0.8 mag in the g band, 20.0 ± 0.8 mag in the r band and

19.8 ± 0.7 mag in the i band, which directly affects the errors on the simulated light curves and therefore their signal-to-noise ratio (S/N).

The new set of data alone, which was characterized by the higher cadence of ZTF Phase II, gives a rate constraint of $R < 1904$ Gpc^{-3} yr^{-1}; combined with the previous analysis, this provides a rate constraint $R < 900$ Gpc^{-3} yr^{-1} for kilonovae similar to GW170817 (95% confidence), using the best-fit model from Dietrich et al. (2020) with dynamic ejecta mass of $m_{\rm dyn}^{\rm ej} = 0.005$ $M_\odot$, disk-wind ejecta mass $m_{\rm wind}^{\rm ej} = 0.050$ $M_\odot$, and opening angle $\Phi = 45°$. This measurement improves our previous limits by 49%. To demonstrate the sensitivity of our results to our assumptions, a limit requiring two or more detections with 5σ significance yields $R_{\rm KN} < 1017$ Gpc^{-3} yr^{-1}, less constraining by a small amount.

We explore the rate constraint under different assumptions on the kilonova population. If all kilonovae were like GW170817 but with a viewing angle uniformly distributed in cosine, the rate constraint becomes $R_{\rm KN} < 2000$ Gpc^{-3} yr^{-1}. We also compute the limits with a more conservative model with a smaller ejecta mass than measured for GW170817; we use a two-component model with dynamic ejecta mass of $m_{\rm dyn}^{\rm ej} = 0.005$ $M_\odot$, disk-wind ejecta mass $m_{\rm wind}^{\rm ej} = 0.010$ $M_\odot$, and opening angle $\Phi = 30°$ (i.e., a factor of 5 less massive disk-wind ejecta). This model provides a limit of $R_{\rm KN} < 1700$ Gpc^{-3} yr^{-1} for a viewing angle fixed to 20° (Mooley et al. 2018); if instead the viewing is allowed to vary, the rate constraint becomes $R_{\rm KN} < 3100$ Gpc^{-3} yr^{-1}.

An upper limit of $R_{\rm KN} < 900$ Gpc^{-3} yr^{-1} for GW170817-like kilonovae is consistent (Figure 8) with the most recent binary neutron star merger rate, inferred from GW observations, of $R_{\rm BNS} = 320_{-240}^{+490}$ Gpc^{-3} yr^{-1} (The LIGO Scientific
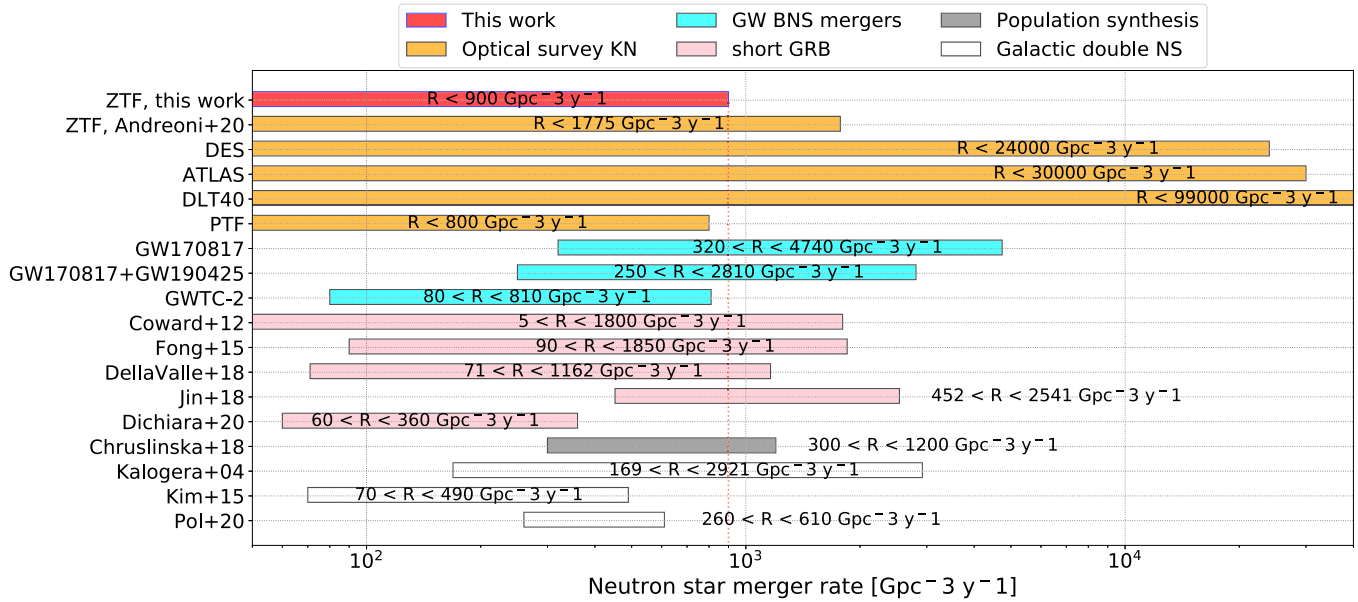
Figure 8. Upper limits on kilonova rates from optical surveys (this work and Andreoni et al. 2020e; Doctor et al. 2017; Kasliwal et al. 2017; Smartt et al. 2017; Yang et al. 2017) compared with binary neutron star merger rates obtained via GW (The LIGO Scientific Collaboration & the Virgo Collaboration 2020a; Abbott et al. 2017b; The LIGO Scientific Collaboration & the Virgo Collaboration 2020b), short GRB (Coward et al. 2012; Fong et al. 2015; Della Valle et al. 2018; Jin et al. 2018; Dichiara et al. 2020), and Galactic double neutron star observations (Kalogera et al. 2004; Kim et al. 2015; Pol et al. 2020), along with population synthesis results (Chruslinska et al. 2018).

Collaboration & the Virgo Collaboration 2020a); our limits may be optimistic as kilonovae may exist that are fainter than GW170817 (for a recent analysis of the kilonova luminosity function based on O3 follow-up observations, see Kasliwal et al. 2020).

6. Conclusions

In this paper, we have presented an overview of `ZTFReST`, an open-source infrastructure built on top of the ZTF alert stream to search for kilonovae and other fast transients. We described how this infrastructure has already yielded a number of candidates, including at least seven confirmed afterglows. Four of these were found during 265 days of science validation on archival searches (ZTF20aajnksq, ZTF20abbiixp, ZTF20abwysqy, ZTF20abtxwfx), two were discovered during real-time operations (ZTF20acozryr and ZTF21aagwbjr), and one was recovered after a parameter optimization of the pipeline (ZTF21aaeyldq). The `ZTFReST` early identification of three of these afterglows, specifically ZTF20abtxwfx, ZTF20acozryr, and ZTF21aagwbjr made it possible to carry out multi-wavelength follow-up observations.

Kilonovae are rapid transients of primary importance for this project. The non-detection of viable kilonovae in the ZTF data set allowed us to constrain the GW170817-like kilonova rate to $R < 900 \ \mathrm{Gpc^{-3} \ yr^{-1}}$. We found that cosmological afterglows (with or without a gamma-ray counterpart) are the dominant *contaminants* for kilonova searches at high Galactic latitude, after cataclysmic variables and flare stars are rejected via accurate vetting. Figure 9 presents a comparison between the rescaled early light curves of the extragalactic fast transients found by `ZTFReST`, the GW170817 kilonova, and the fast blue optical transient (FBOT) AT2018cow. This shows the potential of `ZTFReST` for serendipitous afterglow discovery, i.e., independent of gamma-ray triggers. More of such discoveries could eventually shed some light on the puzzling paucity of *dirty fireballs* and *orphan* GRB afterglows (Dermer et al. 2000;
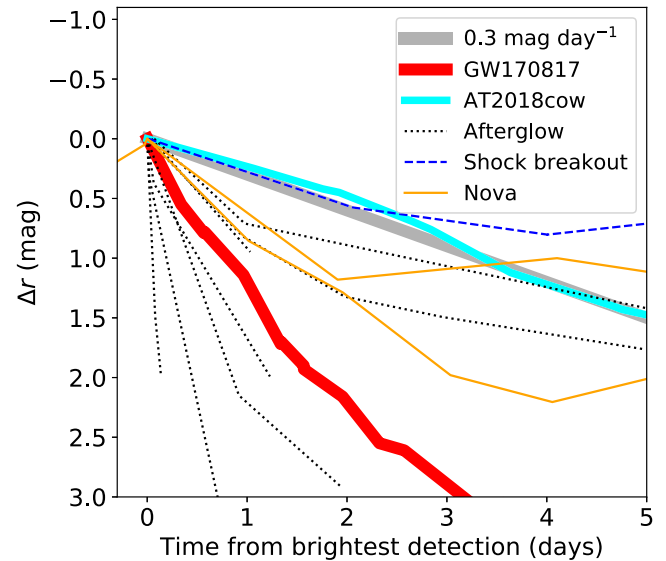
Figure 9. Evolution in the *r* band of extragalactic fast transients found by `ZTFReST`, compared with the GW170817 kilonova (data from Arcavi et al. 2017; Kasliwal et al. 2017; Smartt et al. 2017) and the FBOT AT2018cow (data from Perley et al. 2019).

Huang et al. 2002; Rhoads 2003) in optical surveys. Future work will present more details on the afterglows discovered by ZTF, with a discussion on how the event rate compares to expectations for long GRBs and the implications for hypothesized populations of dirty fireballs.

This effort will also inform us about what strategies, both in terms of survey and alert characterization, will improve kilonova searches going forward. For example, both the cadence and filter choices of ZTF can change the stream of transient candidates that passes our thresholds (see also Almualla et al. 2021). In the future, it will be supplemented by machine-learning-based classifiers for transients Stachie et al. (2020); Muthukrishna et al. (2019),

possibly with data-augmentation scheduling decisions based on optimizing science return Sravan et al. (2020).

Future synoptic surveys such as Vera C. Rubin Observatory's LSST will rely on alert streams very similar to ZTF. LSST is expected to produce ∼10 M alerts per night, which presents us with a data mining challenge, but also puts a strain on follow-up telescope resources. While LSST will perform forced photometry on all transients, image-stacking services are currently not planned for LSST, although they could be key to unveiling a population of tens of kilonovae, especially in fields observed with nightly cadence (Andreoni et al. 2019a). Based on results from ZTF, we can expect the application of ZTFReST to the LSST alert stream to yield a manageable number of extragalactic fast transients with a low number of "false positives" outside of the Galactic plane, especially if crossmatch with nearby galaxies is required. Kilonova science with LSST would strongly benefit from cadences, especially new rolling cadences, optimized for detecting more nearby (and therefore brighter) fast transients, easier to follow-up and classify with other telescopes (I. Andreoni et al. 2021, in preparation). A dedicated performance analysis with LSST test alerts, based on DECam optical observations, is planned. The transients found by LSST and selected with ZTFReST can then be prioritized for rapid characterization with large telescopes. This approach may represent the scientifically crucial divide between candidate *detection* and transient *discovery* in the LSST era.

Software: Astropy (Astropy Collaboration et al. 2013); CASA (McMullin et al. 2007); HEALPix (Górski et al. 2005); simsurvey (Feindt et al. 2019).

ORCID iDs

Igor Andreoni ⬤ https://orcid.org/0000-0002-8977-1498
Michael W. Coughlin ⬤ https://orcid.org/0000-0002-8262-2924
Erik C. Kool ⬤ https://orcid.org/0000-0002-7252-3877
Mansi M. Kasliwal ⬤ https://orcid.org/0000-0002-5619-4938
Varun Bhalerao ⬤ https://orcid.org/0000-0002-6112-7609
Ana Sagués Carracedo ⬤ https://orcid.org/0000-0002-3498-2167
Anna Y. Q. Ho ⬤ https://orcid.org/0000-0002-9017-3567
Kritti Sharma ⬤ https://orcid.org/0000-0002-4477-3625
Tomás Ahumada ⬤ https://orcid.org/0000-0002-2184-6430
Shreya Anand ⬤ https://orcid.org/0000-0003-3768-7515
Leo P. Singer ⬤ https://orcid.org/0000-0001-9898-5597
Daniel A. Perley ⬤ https://orcid.org/0000-0001-8472-1996
Eric C. Bellm ⬤ https://orcid.org/0000-0001-8018-5348
Mattia Bulla ⬤ https://orcid.org/0000-0002-8255-5127
Tim Dietrich ⬤ https://orcid.org/0000-0003-2374-307X
Dmitry A. Duev ⬤ https://orcid.org/0000-0001-5060-8733
Ariel Goobar ⬤ https://orcid.org/0000-0002-4163-4996
Matthew J. Graham ⬤ https://orcid.org/0000-0002-3168-0139
David L. Kaplan ⬤ https://orcid.org/0000-0001-6295-2881
S. R. Kulkarni ⬤ https://orcid.org/0000-0001-5390-8563
Russ R. Laher ⬤ https://orcid.org/0000-0003-2451-5482
Ashish A. Mahabal ⬤ https://orcid.org/0000-0003-2242-0244
David L. Shupe ⬤ https://orcid.org/0000-0003-4401-0430
Jesper Sollerman ⬤ https://orcid.org/0000-0003-1546-6615
Yuhan Yao ⬤ https://orcid.org/0000-0001-6747-8509

References

Aasi, J., Abadie, J., Abbott, B. P., et al. 2015, CQGra, 32, 115012
Abbott, B. P., Abbott, R., Abbott, T. D., et al. 2017a, Natur, 551, 85
Abbott, B. P., Abbott, R., Abbott, T. D., et al. 2017b, PhRvL, 119, 161101
Abbott, B. P., Abbott, R., Abbott, T. D., et al. 2017c, ApJL, 848, L13

Acernese, F., Agathos, M., Agatsuma, K., et al. 2015, CQGra, 32, 024001
Ackley, K., Amati, L., Barbieri, C., et al. 2020, A&A, 643, A113
Ahumada, T., Anand, S., Stein, R., et al. 2020, GCN, 28295, 1
Ahumada, T., Singer, L. P., Anand, S., et al. 2021, NatAs, in press (arXiv:2105.05067)
Alexander, K. D., Berger, E., Fong, W., et al. 2017, ApJL, 848, L21
Almualla, M., Anand, S., Coughlin, M. W., et al. 2021, MNRAS, 504, 2822
Anand, S., Coughlin, M. W., Kasliwal, M. M., et al. 2020, NatAs, 5, 46
Andreoni, I., Ackley, K., Cooke, J., et al. 2017, PASA, 34, e069
Andreoni, I., Anand, S., Bianco, F. B., et al. 2019a, PASP, 131, 068004
Andreoni, I., Cooke, J., Webb, S., et al. 2020a, MNRAS, 491, 5852
Andreoni, I., Coughlin, M., Ahumada, T., et al. 2021a, GCN, 29446, 1
Andreoni, I., Coughlin, M., Kool, E., et al. 2021b, TNSAN, 89, 1
Andreoni, I., Goldstein, D. A., Anand, S., et al. 2019b, ApJL, 881, L16
Andreoni, I., Goldstein, D. A., Kasliwal, M. M., et al. 2020b, ApJ, 890, 131
Andreoni, I., Ho, A., Coughlin, M., et al. 2020c, GCN, 28305, 1
Andreoni, I., Ho, A., Coughlin, M., et al. 2020d, ATel, 13978, 1
Andreoni, I., Kool, E. C., Sagués Carracedo, A., et al. 2020e, ApJ, 904, 155
Annala, E., Gorda, T., Kurkela, A., & Vuorinen, A. 2018, PhRvL, 120, 172703
Antier, S., Agayeva, S., Almualla, M., et al. 2020, MNRAS, 497, 5518
Arcavi, I., Hosseinzadeh, G., Howell, D. A., et al. 2017, Natur, 551, 64
Astropy Collaboration, Robitaille, T. P., Tollerud, E. J., et al. 2013, A&A, 558, A33
Bauswein, A., Goriely, S., & Janka, H.-T. 2013, ApJ, 773, 78
Bauswein, A., Just, O., Janka, H.-T., & Stergioulas, N. 2017, ApJL, 850, L34
Belkin, S., Klunko, E., Zhornichenko, A., et al. 2020a, GCN, 28875, 1
Belkin, S., Krugov, M., Kim, V., et al. 2020b, GCN, 28862, 1
Belkin, S., Pankov, N., Pozanenko, A., Klunko, E. & GRB IKI FuN 2020c, GCN, 28883, 1
Belkin, S., Pozanenko, A., Burhonov, O., et al. 2020e, GCN, 29181, 1
Belkin, S., Pozanenko, A., Rumyantsev, V., Pankov, N. & GRB IKI FuN 2020d, GCN, 28886, 1
Bellm, E. C., Kulkarni, S. R., Barlow, T., et al. 2019, PASP, 131, 068003
Berger, E. 2014, ARA&A, 52, 43
Bloemen, S., Groot, P., Nelemans, G., & Klein-Wolt, M. 2015, in ASP Conf. Ser., 496, Living Together: Planets, Host Stars and Binaries, ed. S. M. Rucinski, G. Torres, & M. Zejda (San Francisco, CA: ASP), 254
Bromberg, O., Nakar, E., Piran, T., & Sari, R. 2013, ApJ, 764, 179
Bulla, M. 2019, MNRAS, 489, 5037
Burns, E., Connaughton, V., Zhang, B.-B., et al. 2016, ApJ, 818, 110
Cenko, S. B., Kulkarni, S. R., Horesh, A., et al. 2013, ApJ, 769, 130
Cenko, S. B., Urban, A. L., Perley, D. A., et al. 2015, ApJL, 803, L24
Chambers, K. C., Magnier, E. A., Metcalfe, N., et al. 2016, arXiv:1612.05560
Chandra, P., & Frail, D. A. 2012, ApJ, 746, 156
Chen, T.-W., Yang, S., Pan, Y.-C., et al. 2021, TNSAN, 92, 1
Chornock, R., Berger, E., Kasen, D., et al. 2017, ApJL, 848, L19
Chruslinska, M., Belczynski, K., Klencki, J., & Benacquista, M. 2018, MNRAS, 474, 2937
Cook, D. O., Kasliwal, M. M., Van Sistine, A., et al. 2019, ApJ, 880, 7
Coughlin, M. W., Ahumada, T., Anand, S., et al. 2019d, ApJL, 885, L19
Coughlin, M. W., Ahumada, T., Cenko, S. B., et al. 2019e, PASP, 131, 048001
Coughlin, M. W., Andreoni, I., Anand, S., et al. 2020c, GCN, 28841, 1
Coughlin, M. W., Antier, S., Dietrich, T., et al. 2020b, NatCo, 11, 4129
Coughlin, M. W., Dietrich, T., Antier, S., et al. 2019c, MNRAS, 492, 863
Coughlin, M. W., Dietrich, T., Doctor, Z., et al. 2018, MNRAS, 480, 3871
Coughlin, M. W., Dietrich, T., Heinzel, J., et al. 2020a, PhRvR, 2, 022006
Coughlin, M. W., Dietrich, T., Margalit, B., & Metzger, B. D. 2019a, MNRAS, 489, L91
Coulter, D. A., Foley, R. J., Kilpatrick, C. D., et al. 2017, Sci, 358, 1556
Coward, D. M., Howell, E. J., Piran, T., et al. 2012, MNRAS, 425, 2668
Cowperthwaite, P. S., Berger, E., Villar, V. A., et al. 2017, ApJL, 848, L17
Dálya, G., Galgóczi, G., Dobos, L., et al. 2018, MNRAS, 479, 2374
De, K., Hankins, M. J., Kasliwal, M. M., et al. 2020b, PASP, 132, 025001
De, K., Kasliwal, M. M., Tzanidakis, A., et al. 2020a, ApJ, 905, 58
de Ugarte Postigo, A., Kann, D. A., Perley, D. A., et al. 2021, GCN, 29307, 1
Dekany, R., Smith, R. M., Riddle, R., et al. 2020, PASP, 132, 038001
Del Vecchio, R., Dainotti, M. G., & Ostrowski, M. 2016, ApJ, 828, 36
Della Valle, M., Guetta, D., Cappellaro, E., et al. 2018, MNRAS, 481, 4355
Dermer, C. D., Chiang, J., & Mitman, K. E. 2000, ApJ, 537, 785
Dey, A., Schlegel, D. J., Lang, D., et al. 2019, AJ, 157, 168
Díaz, M. C., Macri, L. M., Garcia Lambas, D., et al. 2017, ApJL, 848, L29
Dichiara, S., Troja, E., O'Connor, B., et al. 2020, MNRAS, 492, 5011
Dietrich, T., Coughlin, M. W., Pang, P. T. H., et al. 2020, Sci, 370, 1450
Dietrich, T., & Ujevic, M. 2017, CQGra, 34, 105014

Doctor, Z., Kessler, R., Chen, H. Y., et al. 2017, ApJ, 837, 57
Drout, M. R., Piro, A. L., Shappee, B. J., et al. 2017, Sci, 358, 1570
Duev, D. A., Mahabal, A., Masci, F. J., et al. 2019, MNRAS, 489, 3582
Evans, P. A., Cenko, S. B., Kennea, J. A., et al. 2017, Sci, 358, 1565
Evans, P. A., Kuin, N. P. M., & Sbarufatti, B. 2020, GCN, 28858, 1
Feindt, U., Nordin, J., Rigault, M., et al. 2019, JCAP, 2019, 005
Fermi GBM Team 2020, GCN, 28254, 1
Flaugher, B., Diehl, H. T., Honscheid, K., et al. 2015, AJ, 150, 150
Fong, W., Berger, E., Margutti, R., & Zauderer, B. A. 2015, ApJ, 815, 102
Fremling, C., Miller, A. A., Sharma, Y., et al. 2020, ApJ, 895, 32
Fremling, C., Sollerman, J., Taddia, F., et al. 2016, A&A, 593, A68
Gehrels, N., Cannizzo, J. K., Kanner, J., et al. 2016, ApJ, 820, 136
Gehrels, N., Chincarini, G., Giommi, P., et al. 2004, ApJ, 611, 1005
Gehrels, N., & Mészáros, P. 2012, Sci, 337, 932
Goldstein, A., Fletcher, C., Veres, P., et al. 2020, ApJ, 895, 40
Goldstein, A., Veres, P., Burns, E., et al. 2017, ApJL, 848, L14
Goldstein, D. A., Andreoni, I., Nugent, P. E., et al. 2019, ApJL, 881, L7
Gomez, S., Hosseinzadeh, G., Cowperthwaite, P. S., et al. 2019, ApJL, 884, L55
Gompertz, B. P., Cutter, R., Steeghs, D., et al. 2020, MNRAS, 497, 726
Górski, K. M., Hivon, E., Banday, A. J., et al. 2005, ApJ, 622, 759
Graham, M. J., Kulkarni, S. R., Bellm, E. C., et al. 2019, PASP, 131, 078001
Haggard, D., Nynka, M., Ruan, J. J., et al. 2017, ApJL, 848, L25
Hallinan, G., Corsi, A., Mooley, K. P., et al. 2017, Sci, 358, 1579
Ho, A. Y. Q., Kulkarni, S. R., Nugent, P. E., et al. 2018, ApJL, 854, L13
Ho, A. Y. Q., Perley, D., & Andreoni, I. 2020a, ATel, 13986, 1
Ho, A. Y. Q., Perley, D. A., Beniamini, P., et al. 2020c, ApJ, 905, 98
Ho, A. Y. Q., Perley, D. A., Yao, Y., Andreoni, I. & Zwicky Transient Facility Collaboration 2021, GCN, 29305, 1
Ho, A. Y. Q., Yao, Y., Perley, D. A. & Zwicky Transient Facility Collaboration 2020b, GCN, 27799, 1
Högbom, J. A. 1974, A&AS, 15, 417
Hotokezaka, K., Nakar, E., Gottlieb, O., et al. 2019, NatAs, 3, 940
Hu, L., Wu, X., Andreoni, I., et al. 2017, SciBu, 62, 1433
Huang, Y. F., Dai, Z. G., & Lu, T. 2002, MNRAS, 332, 735
Hurley, K., Ipn, Mitrofanov, I. G., et al. 2021, GCN, 29408, 1
Ivezić, Ž., Kahn, S. M., Tyson, J. A., et al. 2019, ApJ, 873, 111
Jin, Z.-P., Li, X., Wang, H., et al. 2018, ApJ, 857, 128
Kalogera, V., Kim, C., Lorimer, D. R., et al. 2004, ApJL, 614, L137
Kasen, D., Metzger, B., Barnes, J., Quataert, E., & Ramirez-Ruiz, E. 2017, Natur, 551, 80, EP
Kasliwal, M. M., Anand, S., Ahumada, T., et al. 2020, ApJ, 905, 145
Kasliwal, M. M., Cannella, C., Bagdasaryan, A., et al. 2019a, PASP, 131, 038003
Kasliwal, M. M., Kasen, D., Lau, R. M., et al. 2019b, MNRAS, in press (doi:10.1093/mnrasl/slz007)
Kasliwal, M. M., Nakar, E., Singer, L. P., et al. 2017, Sci, 358, 1559
Kilpatrick, C. D., Foley, R. J., Kasen, D., et al. 2017, Sci, 358, 1583
Kim, C., Perera, B. B. P., & McLaughlin, M. A. 2015, MNRAS, 448, 928
Klebesadel, R. W., Strong, I. B., & Olson, R. A. 1973, ApJL, 182, L85
Kochanek, C. S., Eisenstein, D. J., Cool, R. J., et al. 2012, ApJS, 200, 8
Kool, E., Andreoni, I., Ho, A., et al. 2021, GCN, 29405, 1
Kouveliotou, C., Meegan, C. A., Fishman, G. J., et al. 1993, ApJL, 413, L101
Kulkarni, S. R. 2020, arXiv:2004.0351
Lai, X., Zhou, E., & Xu, R. 2019, EPJA, 55, 60
Law, N. M., Kulkarni, S. R., Dekany, R. G., et al. 2009, PASP, 121, 1395
Lipunov, V. M., Gorbovsky, E., Kornilov, V. G., et al. 2017, ApJL, 850, L1
Lundquist, M. J., Paterson, K., Fong, W., et al. 2019, ApJ, 881, L26
Margalit, B., & Metzger, B. D. 2017, ApJL, 850, L19
Margutti, R., Berger, E., Fong, W., et al. 2017, ApJL, 848, L20
Masci, F. J., Laher, R. R., Rusholme, B., et al. 2019, PASP, 131, 018003
McBrien, O. R., Smartt, S. J., Huber, M. E., et al. 2021, MNRAS, 500, 4213
McCully, C., Hiramatsu, D., Howell, D. A., et al. 2017, ApJL, 848, L32
McMullin, J. P., Waters, B., Schiebel, D., Young, W., & Golap, K. 2007, in ASP Conf. Ser., 376, Astronomical Data Analysis Software and Systems XVI, ed. R. A. Shaw, F. Hill, & D. J. Bell (San Francisco, CA: ASP), 127
Meegan, C., Lichti, G., Bhat, P. N., et al. 2009, ApJ, 702, 791
Metzger, B. D., Piro, A. L., & Quataert, E. 2008, MNRAS, 390, 781
Metzger, M., Djorgovski, S., Kulkarni, S., et al. 1997, Natur, 387, 878
Milisavljevic, D., Weil, K. E., Rupert, J., et al. 2021, ATel, 14320, 1
Mooley, K. P., Deller, A. T., Gottlieb, O., et al. 2018, Natur, 561, 355
Morgan, J. S., Kaiser, N., Moreau, V., Anderson, D., & Burgett, W. 2012, Proc. SPIE, 8444, 84440H

Moskvitin, A. S. & GRB Follow-Up Team 2020, GCN, 28926, 1

Most, E. R., Weih, L. R., Rezzolla, L., & Schaffner-Bielich, J. 2018, PhRvL, 120, 261103

Muthukrishna, D., Narayan, G., Mandel, K. S., Biswas, R., & Hložek, R. 2019, PASP, 131, 118002

Nayana, A. J., & Chandra, P. 2020, ATel, 14049, 1

Nicholl, M., Berger, E., Kasen, D., et al. 2017, ApJL, 848, L18

Nordin, J., Brinnel, V., van Santen, J., et al. 2019, A&A, 631, A147

Norris, J. P., & Bonnell, J. T. 2006, ApJ, 643, 266

Oke, J. B., Cohen, J. G., Carr, M., et al. 1995, PASP, 107, 375

Paek, G. S. H., Im, M., Kim, J., et al. 2020, GCN, 28880, 1

Patterson, M. T., Bellm, E. C., Rusholme, B., et al. 2018, PASP, 131, 018001

Perley, D. A. 2019, PASP, 131, 084503

Perley, D. A., Ho, A. Y. Q., Yao, Y., et al. 2021, arXiv:2103.01968

Perley, D. A., Mazzali, P. A., Yan, L., et al. 2019, MNRAS, 484, 1031

Pian, E., D'Avanzo, P., Benetti, S., et al. 2017, Natur, 551, 67

Planck Collaboration, Abergel, A., Ade, P. A. R., et al. 2014, A&A, 571, A11

Pol, N., McLaughlin, M., & Lorimer, D. R. 2020, RNAAS, 4, 22

Radice, D., Perego, A., Zappa, F., & Bernuzzi, S. 2018, ApJL, 852, L29

Rhoads, J. E. 2003, ApJ, 591, 1097

Rosswog, S., Feindt, U., Korobkin, O., et al. 2017, CQGra., 34, 104001

Rothberg, B., Kuhn, O., Veillet, C., & Allanson, S. 2020, GCN, 28319, 1

Ryan, G., Eerten, H. v., Piro, L., & Troja, E. 2020, ApJ, 896, 166

Savchenko, V., Ferrigno, C., Kuulkers, E., et al. 2017, ApJ, 848, L15

Shappee, B. J., Simon, J. D., Drout, M. R., et al. 2017, Sci, 358, 1574

Sharma, K., Kumar, H., Dorjay, P., et al. 2020, GCN, 28876, 1

Shenoy, V., Bhalerao, V., Andreoni, I., et al. 2020a, GCN, 28355, 1

Shenoy, V., Bhalerao, V., Gupta, A., et al. 2020b, GCN, 28354, 1

Siegel, D. M., & Metzger, B. D. 2017, PhRvL, 119, 231102

Singer, L. P., Kasliwal, M. M., Cenki, S. B., et al. 2015, ApJ, 806, 52

Smartt, S. J., Chen, T. -W., Jerkstrand, A., et al. 2017, Natur, 551, 75

Smith, K. W., Smartt, S. J., Young, D. R., et al. 2020, PASP, 132, 085002

Somiya, K. 2012, CQGra, 29, 124007

Soumagnac, M. T., & Ofek, E. O. 2018, PASP, 130, 075002

Sravan, N., Milisavljevic, D., Reynolds, J. M., Lentner, G., & Linvill, M. 2020, ApJ, 893, 127

Stachie, C., Coughlin, M. W., Christensen, N., & Muthukrishna, D. 2020, MNRAS, 497, 1320

Stalder, B., Tonry, J., Smartt, S. J., et al. 2017, ApJ, 850, 149

Street, R. A., Bowman, M., Saunders, E. S., & Boroson, T. 2018, Proc. SPIE, 10707, 1070711

Svinkin, D., Golenetskii, R., Aptekar, R., et al. 2020, GCN, 28844, 1

Taguchi, K., Kojiguchi, N., & Isogai, K. 2020, ATel, 14204, 1

Tanvir, N. R., Levan, A. J., González-Fernández, C., et al. 2017, ApJL, 848, L27

The LIGO Scientific Collaboration, & the Virgo Collaboration 2020a, ApJL, 913, L7

The LIGO Scientific Collaboration, & the Virgo Collaboration 2020b, ApJL, 892, L3

Tonry, J. L., Denneau, L., Heinze, A. N., et al. 2018, PASP, 130, 064505

Troja, E., Piro, L., van Eerten, H., et al. 2017, Natur, 551, 71

Ursi, A., Pittori, C., Verrecchia, F., et al. 2020, GCN, 28831, 1

Utsumi, Y., Tanaka, M., Tominaga, N., et al. 2017, PASJ, 69, 101

Valenti, S., Sand, D. J., Yang, S., et al. 2017, ApJL, 848, L24

van der Walt, S. J., Crellin-Quick, A., & Bloom, J. S. 2019, JOSS, 4, 1247

Volnova, A., Belkin, S., Pozanenko, A., et al. 2020, GCN, 28925, 1

Watson, D., Hansen, C. J., Selsing, J., et al. 2019, Natur, 574, 497

Xu, D., Izzo, L., Fynbo, J. P. U., et al. 2021, GCN, 29432, 1

Xu, D., Vielfaure, J. -B., Kann, D. A., et al. 2020b, GCN, 28847, 1

Xu, D., Zhu, Z. P., Fu, S. Y., et al. 2020a, GCN, 28846, 1

Yang, S., Valenti, S., Cappellaro, E., et al. 2017, ApJL, 851, L48

Yao, Y., Miller, A., Ho, A., & Perley, D. 2021, GCN, 29673, 1

Yao, Y., Miller, A. A., Kulkarni, S. R., et al. 2019, ApJ, 886, 152

Zackay, B., Ofek, E. O., & Gal-Yam, A. 2016, ApJ, 830, 27

Zhang, Choi. 2008, A&A, 484, 293

Zhu, Z. P., Fu, S. Y., Liu, X., et al. 2020, GCN, 28854, 1